August 2006

p27Kip1 and p130 Cooperate to regulate Hematopoietic Cell Proliferation in Vivo

Inês Soeiro
Hammersmith Hospital

Azim Mohamedali
King's College London

Hanna M. Romanska
Birmingham University

Nicholas C. Lea
King's College London

Emma S. Child
Imperial College School of Medicine

See next page for additional authors

Authors
Inês Soeiro, Azim Mohamedali, Hanna M. Romanska, Nicholas C. Lea, Emma S. Child, Janet Glassford, Stephen J. Orr, Claudia Roberts, Kikkeri N. Naresh, El-Nasir Lalani, David J. Mann, Roger J. Watson, N. Shaun B. Thomas, and Eric W. -F. Lam

MOLECULAR AND CELLULAR BIOLOGY, Aug. 2006, p. 6170–6184 Vol. 26, No. 16
0270-7306/06/$08.00+0 doi:10.1128/MCB.02182-05

$p27^{Kip1}$ and p130 Cooperate To Regulate Hematopoietic Cell Proliferation In Vivo†

Inês Soeiro,[1] Azim Mohamedali,[2] Hanna M. Romanska,[3,4] Nicholas C. Lea,[2] Emma S. Child,[5] Janet Glassford,[1] Stephen J. Orr,[2] Claudia Roberts,[3] Kikkeri N. Naresh,[4] El-Nasir Lalani,[3,4] David J. Mann,[5] Roger J. Watson,[6] N. Shaun B. Thomas,[2] and Eric W.-F. Lam[1]*

Department of Oncology and Cancer Research UK Labs, MRC Cyclotron Building, Imperial College London, Hammersmith Hospital, Du Cane Road, London W12 0NN, United Kingdom[1]; King's College London, Department of Haematological Medicine, The Rayne Institute, 123 Coldharbour Lane, London SE5 9NU, United Kingdom[2]; Department of Pathology, Cancer Studies Division, Birmingham University, Birmingham B15 2TT, United Kingdom[3]; Department of Histopathology, Hammersmith Hospital & Imperial College London, Du Cane Road, London W12 0HS, United Kingdom[4]; Biochemistry Building, Division of Cell and Molecular Biology, Faculty of Life Sciences, Imperial College, South Kensington, London SW7 2AZ, United Kingdom[5]; and Department of Virology, Faculty of Medicine, St. Mary's Campus, Imperial College London, Norfolk Place, London W2 1PG, United Kingdom[6]

Received 10 November 2005/Returned for modification 9 December 2005/Accepted 27 May 2006

To investigate the potential functional cooperation between $p27^{Kip1}$ and p130 in vivo, we generated mice deficient for both $p27^{Kip1}$ and p130. In $p27^{Kip1-/-}$; $p130^{-/-}$ mice, the cellularity of the spleens but not the thymi is significantly increased compared with that of their $p27^{Kip1-/-}$ counterparts, affecting the lymphoid, erythroid, and myeloid compartments. In vivo cell proliferation is significantly augmented in the B and T cells, monocytes, macrophages, and erythroid progenitors in the spleens of $p27^{Kip1-/-}$; $p130^{-/-}$ animals. Immunoprecipitation and immunodepletion studies indicate that p130 can compensate for the absence of $p27^{Kip1}$ in binding to and repressing CDK2 and is the predominant CDK-inhibitor associated with the inactive CDK2 in the $p27^{Kip1-/-}$ splenocytes. The finding that the $p27^{Kip1-/-}$; $p130^{-/-}$ splenic B cells are hypersensitive to mitogenic stimulations in vitro lends support to the concept that the hyperproliferation of splenocytes is not a result of the influence of their microenvironment. In summary, our findings provide genetic and molecular evidence to show that p130 is a bona fide cyclin-dependent kinase inhibitor and cooperates with $p27^{Kip1}$ to regulate hematopoietic cell proliferation in vivo.

For mammalian cells to duplicate, they have to progress through a series of processes that comprise the cell cycle. The retinoblastoma protein (pRB) pathway (i.e., cyclins, CDKs, CDK-inhibitors [CKIs], pRB, and E2F) links the positive and negative proliferative signals to the cell cycle machinery, and this pathway is inactivated in the majority of human cancers (37, 38). Mammalian cells become growth factor independent after passing the restriction point within the G_1 phase of the cell cycle (34). Two families of G_1 cyclins, D-type cyclins (cyclin D1, D2, and D3) and cyclin E (cyclin E1 and E2) (37), and their dependent kinases (CDK4, -6, and -2) control the transition through G_1 into the S phase of the cell cycle. The principal cellular targets of the G_1 cyclin-dependent CDKs are the pRB family of pocket proteins, consisting of pRB, p107, and p130. In quiescent cells, hypophosphorylated forms of the pRB-related pocket proteins associate with members of the E2F family of transcription factors, thereby negatively regulating the transcriptional activity of E2F-regulated genes, whose products are important for entry into S phase and DNA synthesis (26). In their active forms, cyclin-CDK complexes hyperphosphorylate pRB-related pocket proteins, converting the proteins into their inactive forms. The activities of CDKs are negatively regulated by the CKIs, including the CIP/KIP family of CKIs ($p21^{Cip1/Waf1}$, $p27^{Kip1}$, and $p57^{Kip2}$) that target a broad spectrum of CDKs and the INK4 family of CKIs ($p15^{Ink4b}$, $p16^{Ink4a}$, $p18^{Ink4c}$, and $p19^{Ink4d}$) that specifically inhibits cyclin D-CDK4/ CDK 6 interaction (37). In addition to their roles as CKIs, low levels of $p21^{Cip1}$ and $p27^{Kip1}$ also function to promote the assembly of CDK4 (or CDK6) with the D-type cyclins (3).

Hematopoietic cell number is maintained by the balance between proliferation, differentiation, and death by apoptosis (35, 39). The perturbation of this equilibrium can lead to hematopoietic disorders, including autoimmune diseases, leukemias, and other myeloproliferative and lymphoproliferative disorders (35). Most of the hematopoietic progenitor and mature blood cells are relatively short lived, as they are constantly eliminated by apoptosis. To compensate for this high rate of cell loss, the hematopoietic system requires the production of 10^{11} human (or 10^8 mouse) cells each day. Besides this routine turnover, hematopoietic cell proliferation is also required at times of physiological stress. For example, red blood cell numbers increase under conditions of hypoxia, while granulocyte, macrophage, and lymphocyte populations expand during infections.

The cell cycle is under stringent control during hematopoi-

* Corresponding author. Mailing address: Department of Oncology and Cancer Research UK Labs, MRC Cyclotron Building, Imperial College London, Hammersmith Hospital, Du Cane Road, London W12 0NN, United Kingdom. Phone: 44-20-8383-5829. Fax: 44-20-8383-5830. E-mail: eric.lam@imperial.ac.uk.

† Supplemental material for this article may be found at http://mcb.asm.org/.

etic cell development (14, 40). Restricting access into the cell cycle can help preserve the hematopoietic stem cell and progenitor populations from exhaustion. CKIs, including $p21^{Cip1}$ and $p27^{Kip1}$, are believed to set the stoichiometric thresholds for cell cycle entry in response to mitogenic stimuli, such as cytokines and interactions with stromal cells and the extracellular matrix. $p21^{Cip1}$ and $p27^{Kip1}$ have been shown to maintain the quiescence of hematopoietic stem cells and progenitor cells, respectively, thereby governing their pool sizes (4, 5). In addition, $p27^{Kip1}$ has been demonstrated to negatively regulate the cell cycle entry of some of the more mature hematopoietic cells. However, recent mouse gene deletion studies show that, despite a pronounced lymphoid hyperplasia in thymus and spleen, *p27*$^{Kip1-/-}$ mice do not display overt hematopoietic proliferative abnormalities, indicating that other negative regulators must become activated to compensate for and to maintain hemopoietic cell numbers. Nevertheless, it is unlikely that the function of $p27^{Kip1}$ is substituted by the structurally related Cip/Kip-family of CKIs, as $p57^{Kip2}$ is not normally expressed at significant levels in most hematopoietic cells (29) and recent work with *p21*^{Cip1}-null mice suggested that $p21^{Cip1}$ does not have a role in controlling the proliferation of hematopoietic progenitors and more mature blood cells (4, 5).

A recent study proposed that p130 can function as a CDK2 inhibitor and can compensate for the loss of $p27^{Kip1}$ in *p27*^{Kip1}-null murine embryonic fibroblasts (MEFs) to inhibit CDK2 activity (8, 10). In MEFs with both $p27^{Kip1}$ and p130 deleted, cyclin E-Cdk2 kinase activity cannot be inhibited by mitogen starvation in vitro. It is therefore possible that the lack of overt hematopoietic proliferative disorders in the *p27*$^{Kip1-/-}$ mice is due to functional compensation by the pRB-related p130 protein. However, there have been no data available to suggest that this compensatory mechanism occurs in vivo. To investigate this possibility, we crossbred the mice with *p27*^{Kip1} and *p130* deleted to generate mice deficient for both $p27^{Kip1}$ and p130 in order to study whether the proteins have overlapping roles in proliferative control. Since previous data from an analysis of *p27*$^{Kip1-/-}$ mice showed that $p27^{Kip1}$ is a specific proliferative regulator for hematopoietic organs, including thymus and spleen (15, 23, 32), we therefore focused our study on the effects of this *p27*^{Kip1} and *p130* double deletion in these hematopoietic organs, where $p27^{Kip1}$ has a distinct antiproliferative role.

MATERIALS AND METHODS

Mice breeding and genotyping. The *p130*$^{-/-}$ and *p27*$^{Kip1-/-}$ singly deficient mice have been described previously (9, 15) and were kindly provided by Jim M. Roberts (Howard Hughes Medical Institute, Seattle, WA) and Nicholas J. Dyson (Massachusetts General Hospital Cancer Research Center, Boston, MA). These mice were backcrossed into the C57BL/6 background for two generations and housed at the Imperial College's animal facilities. Double-knockout (DKO) mice, generated by interbreeding *p130*$^{-/-}$ and *p27*$^{Kip1+/-}$ animals, were maintained with the single-knockout mice and the wild-type (WT) controls in the same background within the same colony. Initial crosses of the single-mutant mice yielded *p27*$^{Kip1+/-}$; *p130*$^{+/-}$ animals, which were subsequently intercrossed for a number of generations to eventually generate the breeding pairs consisting of *p27*$^{Kip1-/-}$; *p130*$^{-/-}$ male and *p27*$^{Kip1+/-}$; *p130*$^{-/-}$ female animals. We had to use *p27*$^{Kip1+/-}$; *p130*$^{-/-}$ female mice for breeding, as the female animals with *p27*^{Kip1} homozygous deletions are sterile (15, 23, 32). All mice were used at 8 to 12 weeks of age unless specified otherwise. The genotypes of the mice were determined by PCR using genomic DNA extracted from tail biopsy specimens. The genomic DNA was obtained using the QIAGEN DNeasy tissue kit according to the manufacturer's instructions. The PCR primers are as follows: $p27^{Kip1}$-mutant sense, 5′-TGG AAC CCT GTG CCA TCT CTA T-3′; mutant antisense, 5′-CCT TCT ATC GCC TTC TTG ACG-3′; wild-type sense, 5′-GAT GGA CGC CAG ACA AGC-3′; wild-type antisense, 5′-CTC CTG CCA TTC GTA TCT GC-3′; p130 common, 5′-ACG GAT GTC AGT GTC ACG-3′; wild type, 5′-TAC ATG GTT TCC TTC AGC GG-3′; and mutant, 5′-GAA GAA CGA GAT CAG CAG-3′. All PCRs were carried out in the presence of 2.5 mM $MgCl_2$ at 55°C. Analysis of the PCR products was performed on a standard 2% (wt/vol) agarose gel.

Hematopoietic cell isolation and staining. Mice were sacrificed, and their bone marrow, spleens, and thymi were removed. From these hematopoietic organs, single-cell suspensions were prepared in RPMI 1640 medium by pipetting and then passing through a 70-μm nylon mesh. Cells were washed in phosphate-buffered saline (PBS) containing 0.2% bovine serum albumin, and an aliquot was taken for cell counting in a trypan blue (Sigma, Poole, United Kingdom) exclusion assay. Cells were pelleted by centrifugation for the preparation of whole-cell extracts. For the isolation of lineage-specific hematopoietic cells, cells were sequentially incubated with Miltenyi immunomagnetic microbeads specific for B220 (B cells), Gr1 (monocytes plus macrophages), or Ter-119 (erythroid cells). CD3-positive cells (T cells) were initially stained for 15 min with CD3-fluorescein isothiocyanate (FITC) as described above, followed by staining with anti-FITC immunomagnetic microbeads. Different lineages captured with the microbeads were isolated using the AutoMACS cell sorter (Miltenyi Biotec Ltd., Surrey, United Kingdom) in a two-column purification program specified by the manufacturer. Half of the positive fraction was stained using the appropriate antibody to test for hematopoietic lineage purity, and the other half was fixed for cell cycle analysis. In general, the purity of the lineage-specific cells obtained was >90%, as verified by flow cytometric analysis. For the quantification of lineage-specific hematopoietic cells, nucleated cells from spleens were labeled with lineage-specific antibodies (CD3, B220/CD45R, Gr-1, and Ter-119). The purified monoclonal antibodies anti-CD3ε, phycoerythrin (PE)- or FITC-conjugated anti-B220, PE-conjugated Ter-119, and FITC-conjugated anti-Ly-6G (Gr-1) as well as the respective isotype controls were obtained from BD Pharmingen (Cowley, United Kingdom).

Histological studies and immunohistochemical staining. Following fixation in 10% phosphate-buffered formalin, tissue blocks were dehydrated in graded alcohol by using standard histological techniques, embedded in paraffin, and sectioned with a microtome. Sections were cut for immunohistochemistry onto Snowcoat Xtra slides (Surgipath, Peterborough, United Kingdom). The histological appearance was observed following counterstaining with hematoxylin and eosin (H&E) (Sigma, United Kingdom). Paraffin sections (5 μm) mounted on positively charged glass slides (VWR International, United Kingdom) were processed for conventional histology (H&E) and immunocytochemistry using the avidin-biotin-peroxidase complex (ABC) method (19). Immunocytochemistry for CD3 (rabbit anti-human polyclonal antibody, diluted 1:1,500; Dako, United Kingdom), CD45R/B220 (biotin-conjugated rat anti-mouse monoclonal antibody, diluted 1:1,000; BD Biosciences, United Kingdom), Ter-119 (rat anti-mouse monoclonal antibody, diluted 1:20; BD Pharmingen, United Kingdom), and Gr1 (rat anti-mouse monoclonal antibody, diluted 1:10; eBioscience, United Kingdom) was carried out after antigen retrieval by autoclaving sections at 126°C for 20 min according to the method of Banktlavi and coworkers (1). In brief, following autoclaving, the sections were immersed for 30 min in PBS containing fresh 0.3% (vol/vol) hydrogen peroxide, rinsed in PBS for another 30 min, and incubated for 10 min in normal goat (for CD3) or rabbit (for B220, Ter-119, and Gr1) serum diluted 1:20 in PBS. An incubation with primary antibodies was carried out overnight in a humid chamber at 4°C. The second layer of biotinylated goat anti-rabbit (for CD3) or anti-rat (for Ter-119 and Gr1) serum (1:200; Vector Labs Ltd., Peterborough, United Kingdom) and the third layer of ABC complex (Vector ABC reagent, diluted 1:100) were each applied for 30 min at room temperature. Thorough rinsing in PBS (three 5-min washes) was applied between the sequential steps of the procedure. After a final rinsing in PBS, the sections were developed and counterstained with hematoxylin. Microscopic images were captured using an Olympus DP70 camera (Shinjuku-ku, Tokyo, Japan). As a negative control for the immunostaining, nonimmune serum was used as a first layer.

B-cell isolation and culture. Splenic B cells were prepared by previously published methods (22). Briefly, T cells were killed by a cocktail of monoclonal antibodies against Thy-1, CD4, and CD8 plus guinea pig complement (25). Small, dense B cells were then isolated on Percoll density gradients, and erythrocytes were depleted by treatment with a lysis solution consisting of 0.15 M NH_4Cl. These preparations typically consisted of >95% B lymphocytes. The cells were cultured at 10^5 cells per 100 μl in RPMI 1640 medium supplemented with 5% fetal calf serum, 2 mM glutamine, 100 U/ml penicillin-streptomycin, and 50

μM 2-mercaptoethanol and stimulated with either 10 μg/ml of polyclonal anti-immunoglobulin M (IgM) [affinity-purified $F(ab')_2$ goat anti-mouse IgM (Cappel-ICN, Costa Mesa, CA)] or lipopolysaccharide (LPS) (*Escherichia coli* serotype O55:B5; Sigma, Poole, United Kingdom), 100 U/ml interleukin-4 (IL-4) (R&D Systems, Abingdon, United Kingdom), 10 μg/ml anti-CD40 (clone 3/23) (25), IL-4 plus anti-IgM, anti-CD40 plus anti-IgM, or IL-4 plus anti-CD40. Cells were collected at times indicated for poststimulation.

Cell cycle analysis. Cell cycle analyses were performed by combined propidium iodide (PI) (Sigma) and FITC (Sigma) staining as described previously (43). Briefly, cells were washed with PBS and fixed in 90% ethanol-10% PBS. Following fixation, cells were washed again and then incubated with 50 μg ml^{-1} DNase-free RNase (Sigma), 50 μg ml^{-1} PI, and 0.1 μg ml^{-1} FITC for 30 min at 37 C prior to analysis using a FACSCalibur flow cytometer (Becton Dickinson, Cowley, United Kingdom).

Western blot analysis and antibodies. Western blot whole-cell extracts were prepared by lysing cells with four times the packed cell volume of lysis buffer (1% Nonidet P-40, 100 mM NaCl, 20 mM Tris [pH 7.4], 10 mM NaF, 1 mM sodium orthovanadate, and protease inhibitors (Complete; Roche, Welwyn Garden City, United Kingdom) on ice for 15 min. The protein yield was quantified by using a DC protein assay kit (Bio-Rad, Hemel Hempstead, United Kingdom). A total of 50 μg of lysate was separated by sodium dodecyl sulfate (SDS)-polyacrylamide gel electrophoresis, transferred to nitrocellulose membranes and recognized by specific antibodies. The antibodies against cyclin D2 (M-20), cyclin D3 (18B6-10), cyclin E (M-20), CDK2 (M2), CDK4 (C-22), CDK6 (C-21), $p27^{Kip1}$ (C-19), p107 (C-18), and pRB (C-15) were purchased from Santa Cruz Biotechnology (Santa Cruz, CA). The anti-phospho pRB (Ser807/811) antibody was purchased from Cell Signaling Technologies (Hitchin, United Kingdom), and the anti-phospho pRB (Thr821) antibody was from Biosource International (Camarillo, CA). The anti-p130 (anti-pRB2) (K25020) monoclonal antibodies were acquired from Transduction Laboratories (Cambridge, United Kingdom). The antibodies were detected by using horseradish peroxidase-linked goat anti-mouse or anti-rabbit IgG (Dako, Ely, United Kingdom) or mouse-absorbed goat anti-rat IgG (Southern Biotechnology Associates, Inc.) and visualized by an enhanced chemiluminescence detection system (Amersham Pharmacia Biotech, Amersham, United Kingdom).

Immunoprecipitation, CDK kinase assays, and immunodepletion. For the immunoprecipitation and CDK kinase assays, the cells collected were washed with PBS and lysed in lysis buffer containing 20 mM Tris-HCl (pH 7.9), 150 mM NaCl, 1 mM EGTA, 1 mM EDTA (pH 8.0), 1% Triton X-100, 2.5 mM sodium pyrophosphate, 1 mM sodium orthovanadate, 1 mM phenylmethylsulfonyl fluoride. Protein lysates (100 μg) were then incubated with 5 μg of anti-CDK2 (M-2) for 2 h at 4°C. At 2 h, 50% protein A-Sepharose beads (20 μl; Amersham Pharmacia Biotech) in lysis buffer were added and the mixture was incubated for an additional 2 h. The anti-CDK2 immunoprecipitates were then washed substantially and resuspended in 20 μl of kinase buffer (20 mM Tris-HCl [pH 8.0], 10 mM $MgCl_2$, 1 mM EDTA, 1 mM dithiothreitol) supplemented with 2.5 μg of recombinant pRB protein and 10 μCi of [γ-^{32}P]ATP (3,000 Ci/mmol; Amersham Pharmacia Biotech). Reaction mixtures were incubated for 15 min at room temperature, and the phosphorylated recombinant pRB protein was resolved with 10% SDS-polyacrylamide gel electrophoresis. The gels were then dried and exposed to X-ray films. From isolated $B220^+$ and $CD3^+$ cells, immunoprecipitation kinase assays were performed as described previously (21), except that cells were lysed in 20 mM Tris-HCl (pH 8.0), 250 mM NaCl, 0.5% NP-40, and 1 mM EDTA. For immunodepletion experiments, two extra immunoprecipitations were performed with either the anti-$p27^{Kip1}$ antibody (C-19) or the p130 antibody. The resultant supernatants were resolved on an SDS-polyacrylamide gel electrophoresis gel and analyzed by Western blotting.

[^{3}H]thymidine incorporation assays. Cell proliferation was monitored by [^{3}H]thymidine incorporation assays. Small dense splenic B cells were seeded into 96-well plates at 10^5 cells per well and cultured in 200 μl of RPMI, 0.5 μCi [^{3}H]thymidine, and 10% fetal calf serum. [^{3}H]thymidine was added for the final 4 h of the indicated culture times. Cells were collected using a PHD cell harvester (Cambridge Technology, Cambridge, MA), and [^{3}H]-thymidine incorporation into DNA was quantified by scintillation counting. Each point was determined in quadruplicate, and each growth curve was performed at least three times.

RESULTS

Increase in cell cycle entry and cell number of *p27$^{Kip1-/-}$*; *p130$^{-/-}$* splenocytes. At all stages of interbreeding, the birth of offspring generally obeyed the Mendelian ratio, with the outcomes not statistically different from the predicted values (see Fig. S1 in the supplemental material). However, it was notable that there was a small and nonsignificant ($P = 0.066$) bias against the *p130$^{-/-}$* genotype when we initially crossed p130 heterozygous mice after one generation of backcrossing into a C57BL/6 background. Nevertheless, most of our later crosses using mice after two generations of backcrossing into C57BL/6 showed that births obey the predicted Mendelian ratios. The reason for this bias is unclear, but it could be due to the fact that p130 knockouts in some backgrounds, including BALB/c, are embryonic lethal (28). As a result, mice having had two generations of backcrossing will have an enriched C57BL/6 background, which has been shown to protect offspring from the lethal effects of *p130* deletion (28). Our breeding also showed that *p27$^{Kip1-/-}$*; *p130$^{-/-}$* mice are viable, but there was an apparent higher mortality rate among *p27$^{Kip1-/-}$*; *p130$^{-/-}$* mice (8.7%; 26 deaths among 298 mice within the first 9 months) compared with those of their *p27$^{Kip1-/-}$* (2.5%; 4/120), *p130$^{-/-}$* (4.4%; 3/68), and wild-type (2.5%; 3/132) counterparts; however, the causes of the deaths were unknown. Like *p27$^{Kip1-/-}$* animals, *p27$^{Kip1-/-}$*; *p130$^{-/-}$* mice have higher body weights than wild-type and *p130$^{-/-}$* mice of the same ages (see Fig. 2B). Nevertheless, there is no significant difference in body weight between *p27$^{Kip1-/-}$* and *p27$^{Kip1-/-}$*; *p130$^{-/-}$* mice. As reported, the *p130$^{-/-}$* mice develop normally and have body weights similar to those of wild-type mice. Consistent with previous reports, the $p27^{Kip1-/-}$ mice display organomegaly and infertility and these phenotypes are retained in *p27$^{Kip1-/-}$*; *p130$^{-/-}$* mice.

To investigate the effects of $p27^{Kip1}$ and/or p130 deletion on the proliferation of hematopoietic cell populations, we first studied the cell cycle distribution of nucleated cells isolated directly from the thymus and spleen of the wild-type as well as the singly and doubly deficient mice (Fig. 1A). To this end, cells prepared from these hematopoietic organs were analyzed by flow cytometry following propidium iodide and FITC staining (17, 25). The results showed that the cell cycle profiles of cells from both the spleen and thymus of *p130$^{-/-}$* mice are similar to those of their wild-type counterparts. However, there were marginal increases in S- and G_2/M-phase cells in the thymus and the spleen of *p27$^{Kip1-/-}$* mice. Even higher percentages of S and G_2/M cells were observed in the *p27$^{Kip1-/-}$*; *p130$^{-/-}$* animals, with the increase more obvious in the spleen than in the thymus (Fig. 1B). Despite the large error range for the S- and G_2/M-phase splenic cells in the *p27$^{Kip1-/-}$*; *p130$^{-/-}$* animals, the difference between *p27$^{Kip1-/-}$* and *p27$^{Kip1-/-}$*; *p130$^{-/-}$* groups is significant (t test; $P < 0.01$). These results suggested that both $p27^{Kip1}$ and p130 function in the same proliferation regulatory pathway and that p130 compensates for the absence of $p27^{Kip1}$ in the spleen of the $p27^{Kip1}$-null mice to negatively control cell cycle entry.

The spleens from the *p27$^{Kip1-/-}$*; *p130$^{-/-}$* animals were larger (Fig. 2A) and heavier (Fig. 2B) and had averages of five and three times more cells than those from wild-type (*p130$^{-/-}$*) and *p27$^{Kip1-/-}$* animals, respectively (Fig. 2C). Both of the single-knockout mice also harbored spleens that were larger, with a higher number of cells than those of the wild-type, but to a lesser extent than did the double-knockout mice. This evidence confirms previous reports (15, 23, 32) that stated that the $p27^{Kip1}$-null mice exhibited higher cellularity than

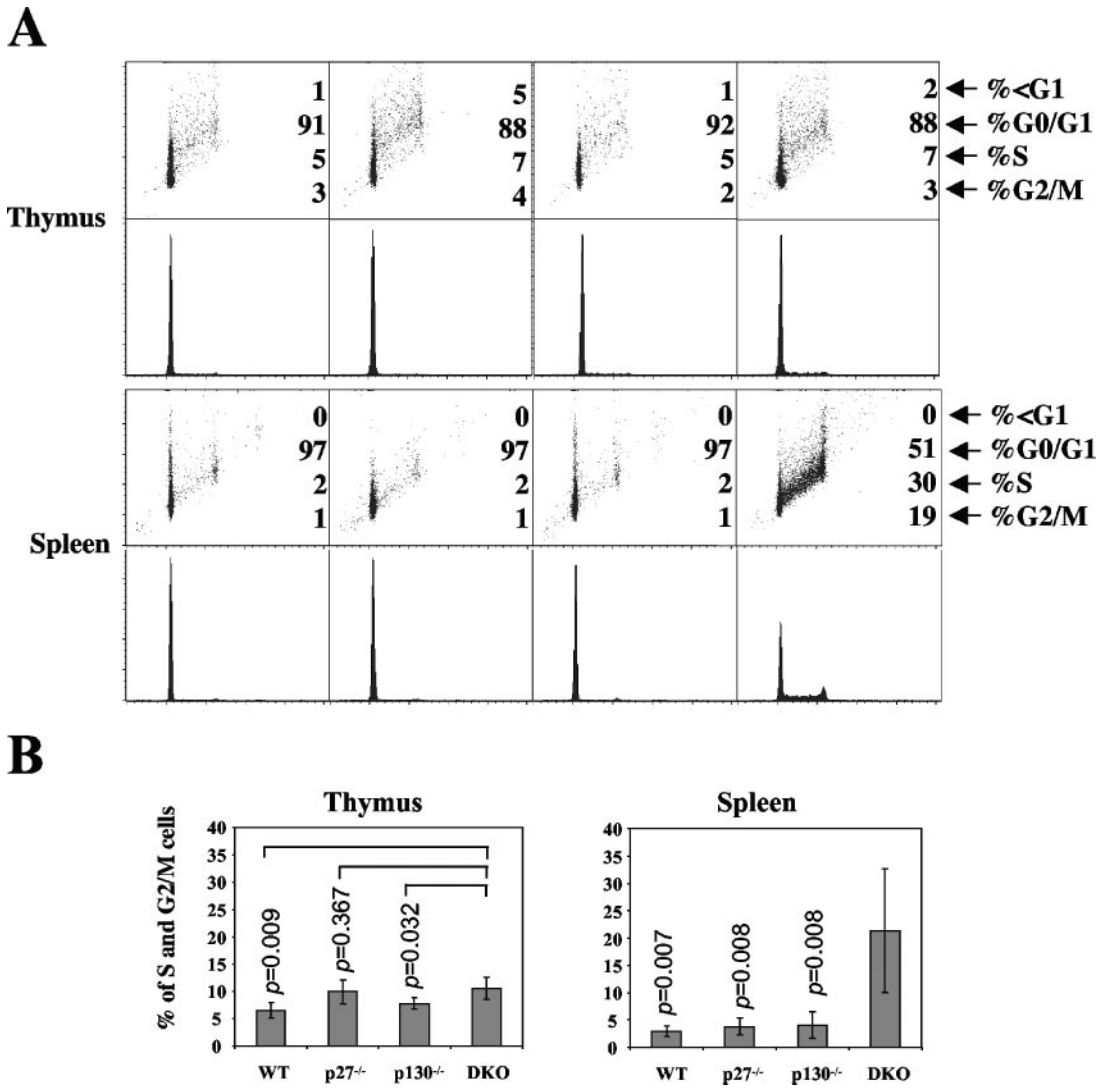

FIG. 1. Cell-cycle analysis of hematopoietic cells from wild-type, $p27^{Kip1-/-}$, $p130^{-/-}$, or $p27^{Kip1-/-}$; $p130^{-/-}$ mice. Nucleated splenic or thymic cells from WT, $p27^{Kip1-/-}$, $p130^{-/-}$, or $p27^{Kip1-/-}$; $p130^{-/-}$ DKO mice were permeabilized and stained with PI and FITC to measure DNA (*x* axis) and protein (*y* axis) content, respectively, and measured by flow cytometry. (A) A representative cell cycle analysis in which the percentage of cells in each phase of the cell cycle (sub-G_1 [$<G_1$], G_0/G_1, S, and G_2/M), determined by their DNA and protein contents, are indicated. (B) The total percentage of cells in S and G_2/M phase of different types of mice is shown in the histogram (mean ± standard deviation [SD]; $n > 12$). Student *t* tests were performed between the DKO samples and the WT, $p27^{Kip1-/-}$, or $p130^{-/-}$ samples. There is a statistically significant difference between the DKO group and the other genotypes ($P < 0.01$) in the spleen but not the thymus.

wild-type mice in several hematopoietic organs, including the spleen and thymus.

Sections from spleen and thymus were studied from four sets of mice (wild-type, $p27^{Kip1-/-}$, $p130^{-/-}$, and $p27^{Kip1-/-}$; $p130^{-/-}$) (Fig. 3). There were no significant differences in thymus upon morphological evaluation (data not shown). Compared to other groups, spleens from $p27^{Kip1-/-}$; $p130^{-/-}$ showed expanded red pulp containing predominantly erythroid and myeloid compartments. The red pulp-to-white pulp (consisting of primarily lymphoid cells) ratio among the $p27^{Kip1-/-}$; $p130^{-/-}$ group was more than 1.5, while among the other groups it was less than 0.75. Furthermore, the density of nucleated cells in the red pulp was four to five times higher in the $p27^{Kip1-/-}$; $p130^{-/-}$ group than in the wild type. Among $p27^{Kip1-/-}$ and $p130^{-/-}$ mice, the cell density in the red pulp was 1.5 to 3 times that of the wild type. The expanded red pulp of the $p27^{Kip1-/-}$; $p130^{-/-}$ mice showed trilineage hematopoiesis in the form of groups of nucleated erythroid cells, maturing myeloid precursors, and occasional megakaryocytes. Although this was best appreciated in the $p27^{Kip1-/-}$; $p130^{-/-}$ mice, mice from other groups also had trilineage hematopoiesis, but this was of a lesser volume and proportion.

To identify the cell populations responsible for this spleen hyperplasia in the $p27^{Kip1}$- and p130-deficient mice, we used microbeads to separate the T and B lymphocytes, the granulocytes plus monocytes, and the erythroid cells from 8- to 9-week-old mice and analyzed their respective cell cycle statuses (S+G_2/M percent) by staining with propidium iodide

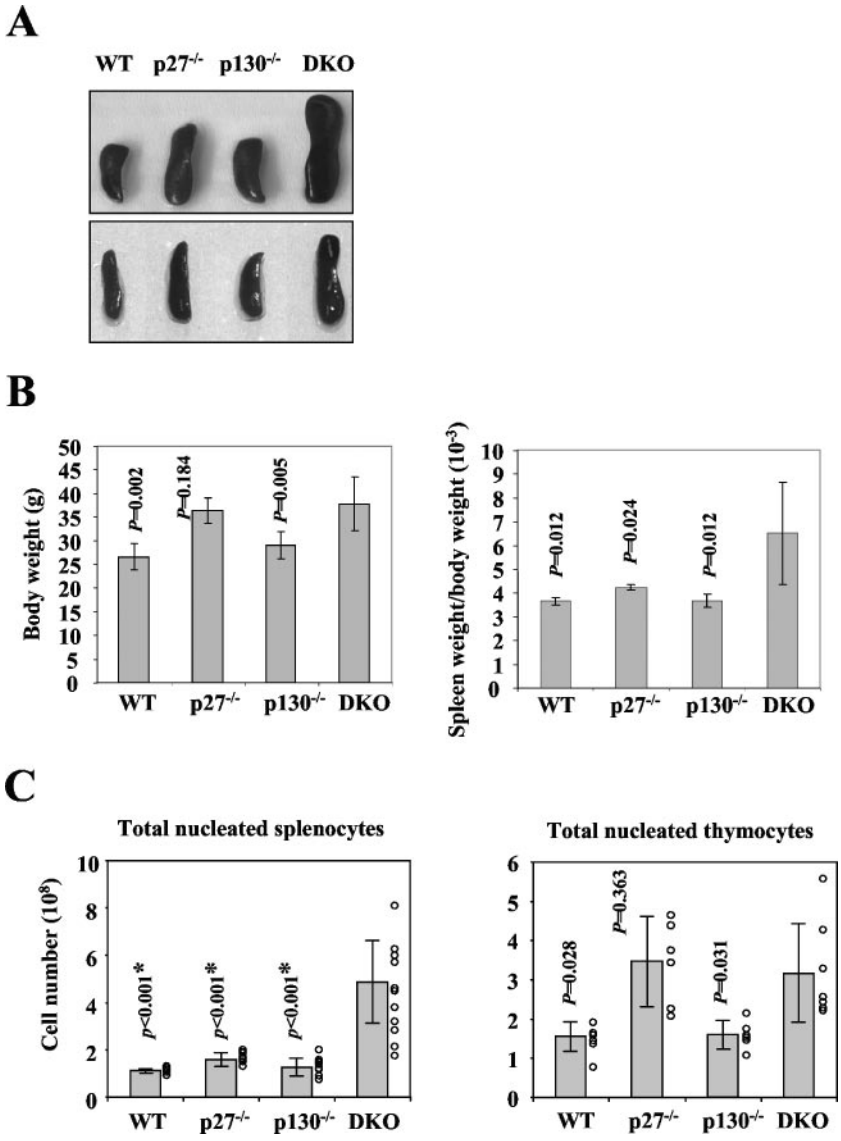

FIG. 2. Comparisons of spleen sizes and cellularities between wild-type, $p27^{Kip1-/-}$, $p130^{-/-}$, and $p27^{Kip1-/-}$; $p130^{-/-}$ mice. (A) Representative photograph images of spleens from wild-type, $p27^{Kip1-/-}$, $p130^{-/-}$, and $p27^{Kip1-/-}$; $p130^{-/-}$ mice. (B) Histograms showing the average body weights (left panel) and spleen weight/body weight ratios (right panel) from wild-type, $p27^{Kip1-/-}$, $p130^{-/-}$ and $p27^{Kip1-/-}$; $p130^{-/-}$ mice (mean ± SD [error bars]; $n > 6$) (left panel). Student t tests were performed between the DKO group and the WT, $p27^{Kip1-/-}$, or $p130^{-/-}$ group. There is a statistically significant difference in average body weights between the DKO group and the WT or $p130^{-/-}$ groups ($P < 0.01$) but not the $p27^{Kip1-/-}$ group. (C) Histograms showing the average total cell numbers of splenocytes and thymocytes present in wild-type, $p27^{Kip1-/-}$, $p130^{-/-}$, and $p27^{Kip1-/-}$; $p130^{-/-}$ mice (mean ± SD [error bars]; $n > 6$). The individual cell numbers are shown by circles alongside the histograms. There is a statistically significant difference between the DKO group and the other genotypes ($P < 0.01$) in the spleen but not the thymus.

(Fig. 4A and B). Younger mice of a narrower age range were used because of the detection of splenomegaly in older mice and the huge error range of the previous whole-spleen cell cycle experiment (Fig. 1B). In these experiments, we observed an increase in the $S+G_2/M$ percent in all cell types examined, but a particularly higher level of $S+G_2/M$ cells was detected in the Ter-119^+ erythroid population (33) and the $Gr1^+$ population containing granulocytes plus monocytes (31, 46). Consistent with this, we also detected a significant increase in cell number in all splenic cell types, but the increases in the Ter-119^+ and $Gr1^+$ cell populations were again the most dramatic (Fig. 4C).

An increase in $B220^+$, $CD3^+$, Ter-119^+, and $Gr1^+$ cells in the spleens of $p27^{Kip1}$- and p130-deficient animals. To confirm that there was an increase in all of the major hemopoietic cell types in the spleens of *$p27^{Kip1}$*- and *p130*-deficient animals, we performed immunohistochemical staining of spleen sections from four sets of mice (wild type, $p27^{Kip1-/-}$, $p130^{-/-}$, and $p27^{Kip1-/-}$; $p130^{-/-}$) with specific antibodies against B220/CD45R, CD3, Ter-119, and Gr1 (Fig. 5). The results confirmed the earlier H&E staining results and showed that there was an increase in cell numbers of all major hemopoietic cell types (B and T cells, erythroid cells, monocytes, and macrophages) in the spleens of the $p27^{Kip1-/-}$; $p130^{-/-}$ mice compared with

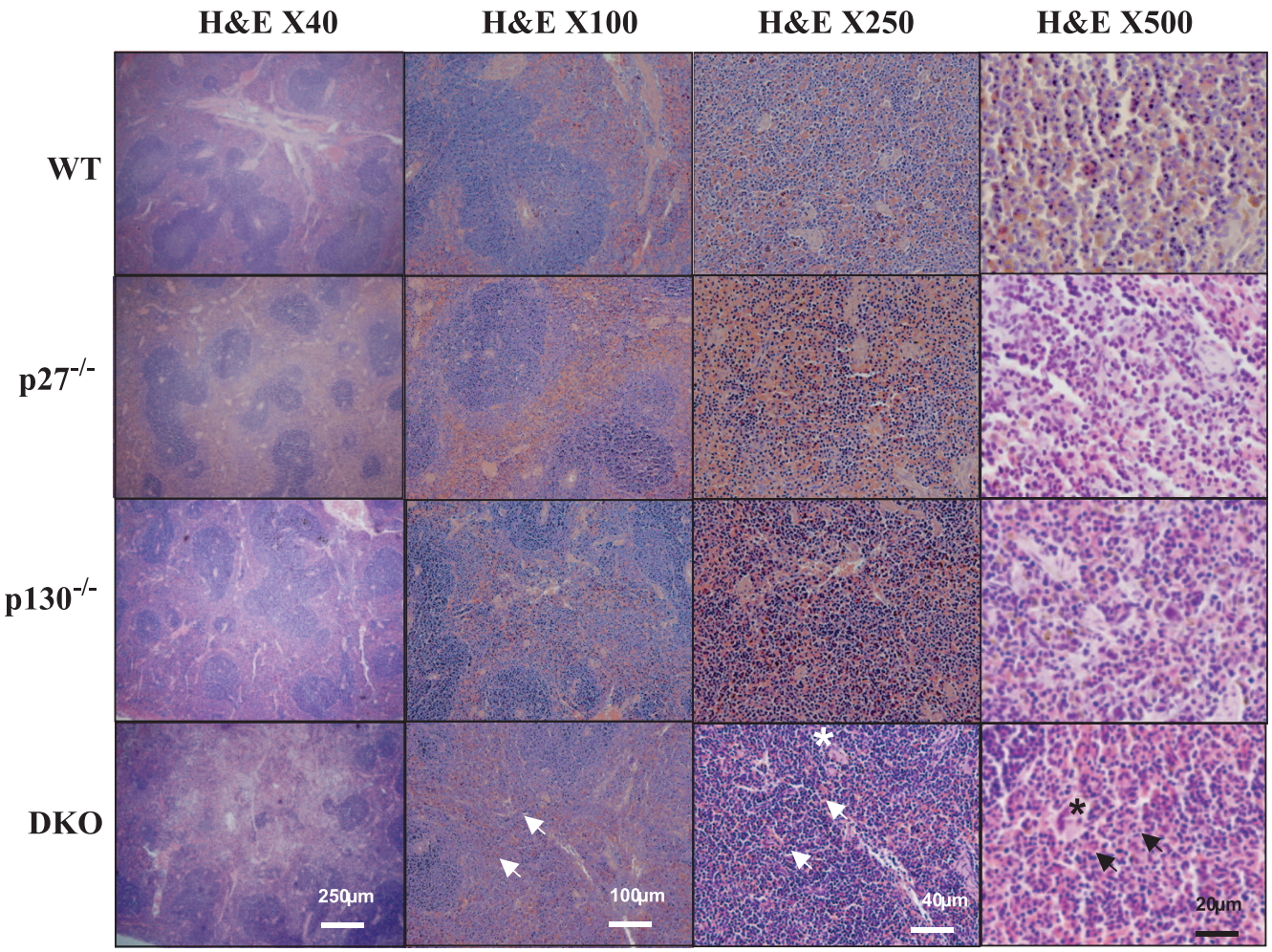

FIG. 3. Hematoxylin and eosin-stained sections of spleens of wild-type, $p27^{Kip1-/-}$, $p130^{-/-}$, and $p27^{Kip1-/-}$; $p130^{-/-}$ mice. Spleen sections from WT, $p27^{Kip1-/-}$, $p130^{-/-}$, and $p27^{Kip1-/-}$; $p130^{-/-}$ DKO mice were stained with H&E. Representative sections were shown ($n = 6$ for each genotype). Mice genotypes and magnifications (×40, ×100, ×250, and ×500) are indicated. Spleen sections from $p27^{Kip1-/-}$; $p130^{-/-}$ mice showed an expanded red pulp. The splenic red pulp of $p27^{Kip1-/-}$; $p130^{-/-}$ mice showed a high cell density. Trilineage hematopoiesis (indicated by arrows) in the form of groups of nucleated erythroid cells, maturing myeloid precursors, and occasional megakaryocytes (indicated by an asterisk) are noted. This is best appreciated in the splenic sections from the $p27^{Kip1-/-}$; $p130^{-/-}$ mice. Scale bars with widths are shown.

their wild-type, $p27^{Kip1-/-}$, and $p130^{-/-}$ counterparts. In the spleens of wild-type mice, the B220/CD45R+ B lineage cells were closely packed in the outer region of the white pulps (lymphoid sheaths). In the spleens of $p27^{Kip1-/-}$, $p130^{-/-}$, and $p27^{Kip1-/-}$; $p130^{-/-}$ mice, the B cells were densely packed towards the inner region, with the highest increase in B-cell number and density observed in the spleens of $p27^{Kip1-/-}$; $p130^{-/-}$ mice. The $CD3^+$ T cells were located predominantly around the central arterioles in the wild-type and spleens of $p130^{-/-}$ mice. The distribution of the $CD3^+$ T cells in spleens of $p27^{Kip1-/-}$ mice was similar to those in the spleens of wild-type and $p130^{-/-}$ mice but had increased density. The density of the $CD3^+$ T cells further increased in the spleens of $p27^{Kip1-/-}$; $p130^{-/-}$ mice, and the $p27^{Kip1-/-}$; $p130^{-/-}$ splenic T cells were located predominantly towards the central region of the lymphoid sheaths. In the spleens of $p27^{Kip1-/-}$, $p130^{-/-}$, and wild-type mice, the Ter-119^+ cells were observed primarily in the peripheral region (lymphoid sheaths) and were of similar densities. The Ter-119^+ cells in the spleens of $p27^{Kip1-/-}$; $p130^{-/-}$ mice were again of a distribution similar to those the other genotypes but were of a much higher density. The immunoreactivity of the Gr1 antibody was weak, which is likely to be due to tissue processing; however, the results also demonstrated that the $Gr1^+$ cells had higher densities and cell numbers in the red pulps of the spleens of $p27^{Kip1-/-}$; $p130^{-/-}$ mice.

Expression of cell cycle regulators in $p27^{Kip1}$- and/or p130-deficient spleens and thymus. The fact that all of the major cell types in the spleens of $p27^{Kip1-/-}$; $p130^{-/-}$ mice displayed increased cell cycle entry allowed us to investigate the molecular mechanism responsible for this hyperproliferative effect by analyzing unfractionated splenocytes. We took advantage of this and examined the expression of cell cycle regulators by Western blot analysis (Fig. 6A). Although most cell cycle regulatory proteins were present at comparable levels in the thymus and the spleen, there was also some variation between

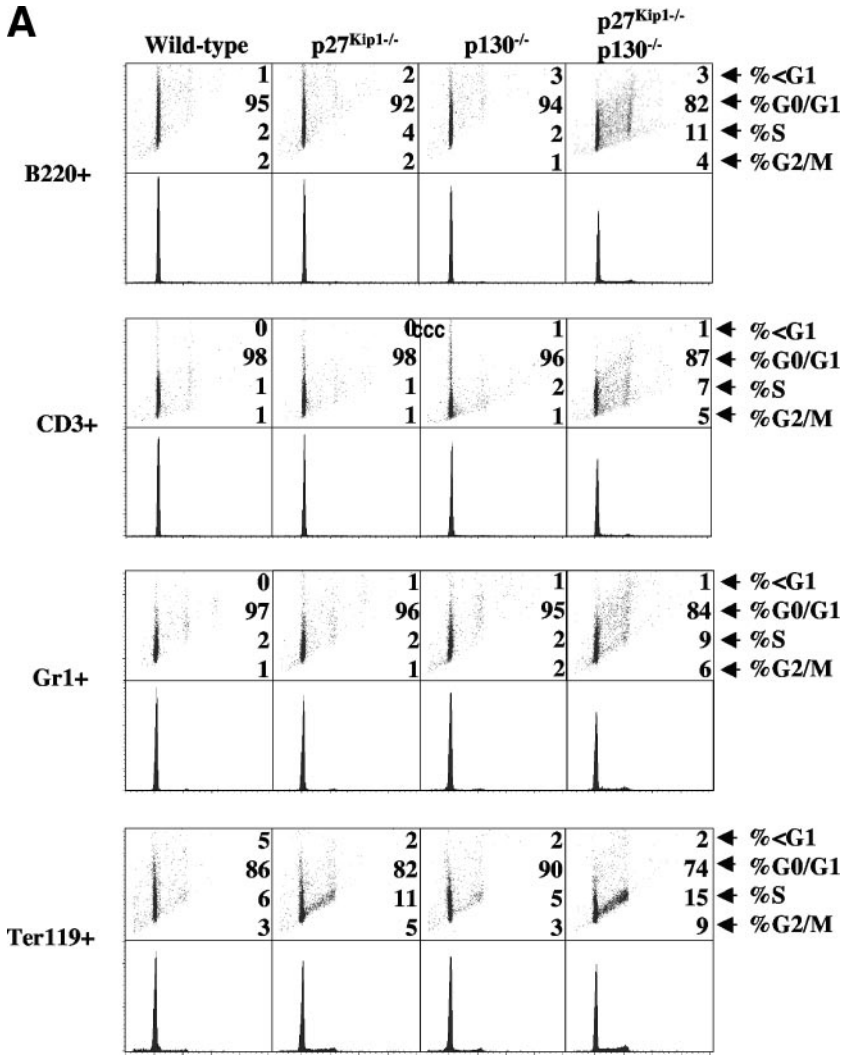

FIG. 4. Cell cycle analysis and cellularity of lineage-specific splenocytes. Nucleated splenocytes were harvested from wild-type, $p27^{Kip1-/-}$, $p130^{-/-}$, and $p27^{Kip1-/-}$; $p130^{-/-}$ mice and sorted according to cell surface markers using immunomagnetic microbeads against B220 (B cells), CD3 (T cells), Gr1 (monocytes plus macrophages), and Ter-119 (erythroid progenitors). These cells were then analyzed for their cell cycle distributions as previously described in the legend for Fig. 1. (A) Representative cell cycle analysis in which the percentage of lineage-specific splenocytes in each phase of the cell cycle (sub-G_1 [$<G_1$], G_0/G_1, S, and G_2/M), as determined by their DNA and protein contents, are indicated. (B) The total percentage of lineage-specific cells in the S and G_2/M phases of different types of 8- to 9-week-old mice is shown in the histogram (mean ± SD [error bars]; $n > 6$). Student t tests were performed between the DKO group and the WT, $p27^{Kip1-/-}$, or $p130^{-/-}$ group. There is a statistically significant difference between the DKO group and the other genotypes ($P < 0.01$). (C) Histograms showing the average cell numbers of lineage-specific splenocytes present in wild-type, $p27^{Kip1-/-}$, $p130^{-/-}$, and $p27^{Kip1-/-}$; $p130^{-/-}$ mice (mean ± SD [error bars]; $n = 6$). The individual cell numbers are shown by circles alongside the histograms. Student t tests were performed between the DKO group and the WT, $p27^{Kip1-/-}$, or $p130^{-/-}$ group. There is a statistically significant difference between the DKO group and the other genotypes ($P < 0.01$).

these two organs. The splenocytes expressed a lower level of CDK6, CDK2, and p107 and a higher level of cyclin D2 compared with the thymocytes. In the spleen, cyclin D2 expression was down-regulated in both the $p27^{Kip1-/-}$ and the $p27^{Kip1-/-}$; $p130^{-/-}$ samples, suggesting a positive role of $p27^{Kip1}$ in cyclin D2 expression. In the spleen of the double-knockout mice, there was also an increase in the expression of p107 and cyclin E and A proteins, which are E2F-regulated gene products and known regulators of the G_1/S and S phases. Since cyclin E and A accumulation is important for passage through the G_1 and S phases, the higher levels of cyclin E and A expression in double-knockout splenocytes compared with that in the wild-type and single-knockout cells explains the greater levels of cell cycle entry and DNA synthesis observed. Since T821 is a CDK2-specific phosphorylation site on pRB and other studies have used T821 pRB phosphorylation as a surrogate for CDK2 activity (27, 45), we therefore used the anti-pRB (T821) phosphospecific antibody to gauge the CDK2 activity. The result showed an increase in CDK2-dependent pRB phosphorylation in the double-knockout splenocytes, indicating an increase in CDK2 activity. The results of Western blot analysis supported the hypothesis that p130 compensates for the loss of $p27^{Kip1}$ in $p27^{Kip1-/-}$ cells to inhibit CDK2 activity. The data also indicated that this compensatory mechanism is specific for spleno-

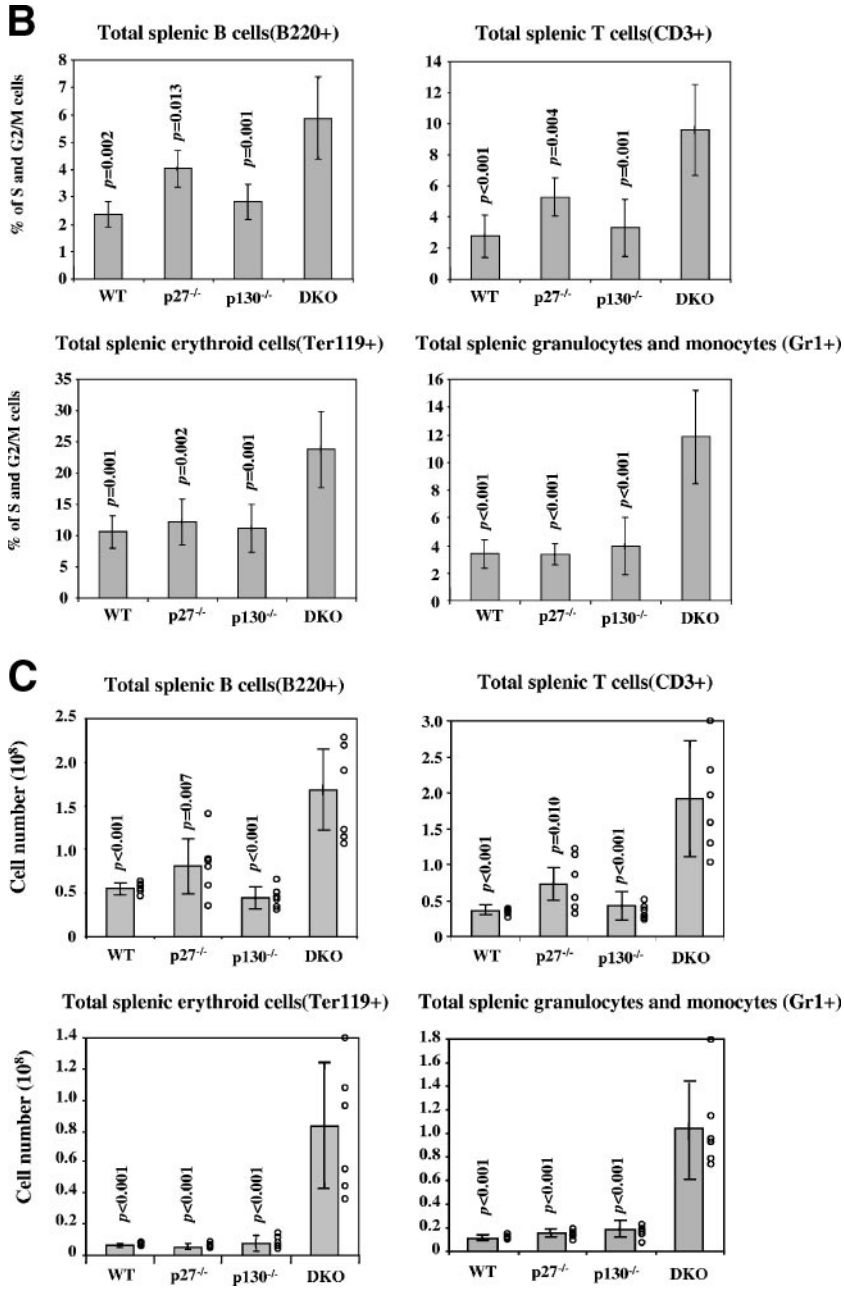

FIG. 4—*Continued.*

cytes, as the induction in CDK2-dependent activity is detected in only splenocytes, not thymic cells and bone marrow cells (data not shown).

CDK2 activity is up-regulated in the p27^{Kip1} and p130 doubly-deficient splenocytes. We next performed immunoprecipitation kinase experiments to confirm the observation that CDK2 activity is up-regulated in the p27^{Kip1} and p130 doubly deficient splenocytes. CDKs were immunoprecipitated from these cells, and the associated kinase activity was measured using a bacterially expressed glutathione *S*-transferase–pRB as a substrate (Fig. 6B). We found that the immunoprecipitated CDK2 but not CDK4 or CDK6 activity is significantly up-regulated (catalytically active) in the *p27^{Kip1}* and *p130* doubly deficient splenocytes but not in their wild-type, *p27$^{Kip1-/-}$*, and *p130$^{-/-}$* counterparts. The data also indicated that CDK2 activity is at a basal level in the splenocytes of *p27$^{Kip1-/-}$* mice, as in the wild-type splenic cells, and this activity is increased through further deletion of p130, suggesting that p130 compensates for the absence of p27^{Kip1} in the spleen cells of *p27$^{Kip1-/-}$* mice to inhibit CDK2 activity. Interestingly, this induction in CDK2 activity was not observed in the *p27$^{Kip1-/-}$*; *p130$^{-/-}$* cells isolated from the thymus, again indicating that this compensatory mechanism by which CDK2 is inhibited is tissue and cell type specific. These results are in agreement

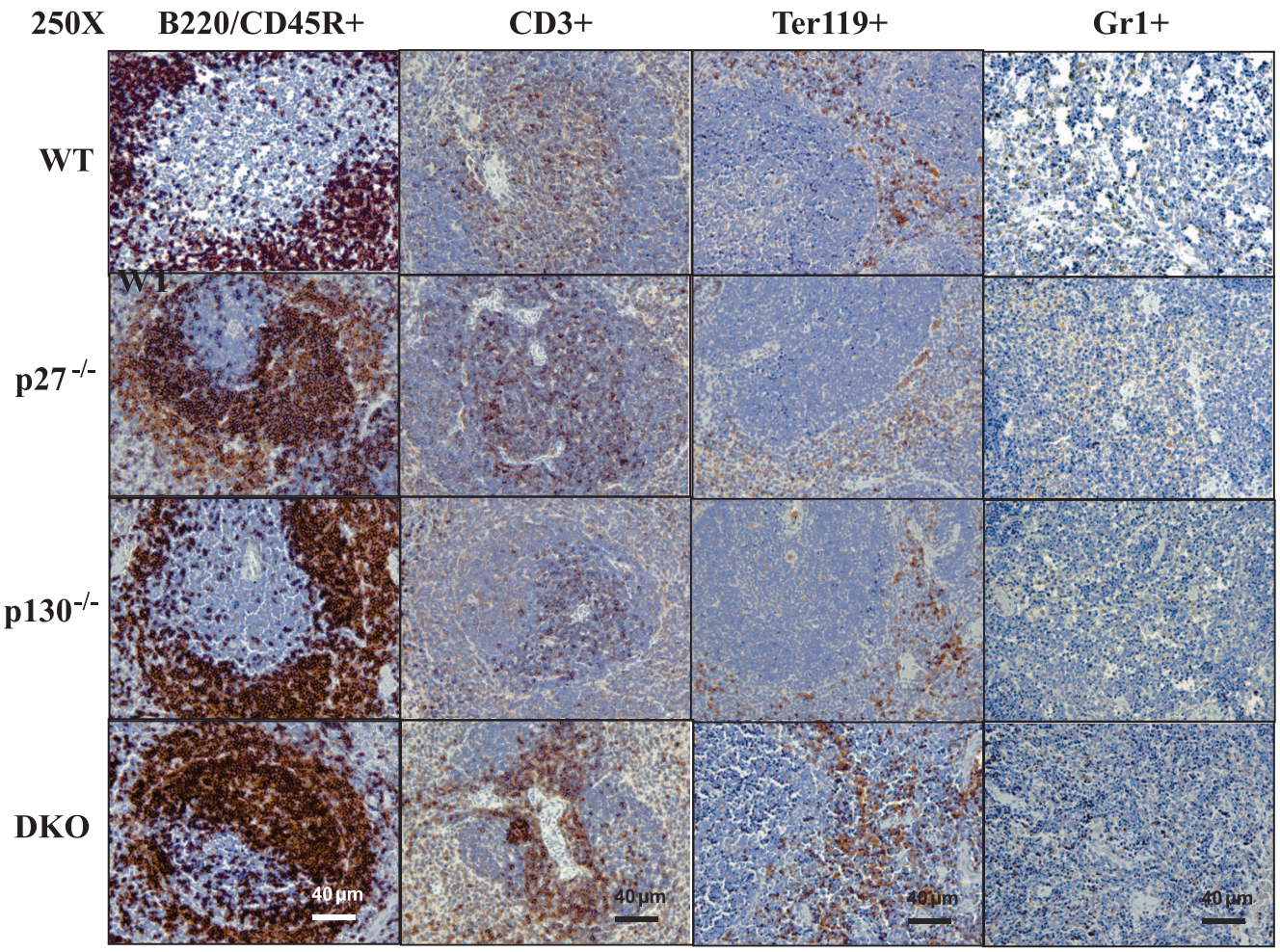

FIG. 5. Sections of wild-type, $p27^{Kip1-/-}$, $p130^{-/-}$, and $p27^{Kip1-/-}$; $p130^{-/-}$ spleens stained with antibodies against B220/CD45R, CD3, Ter-119, and Gr1. Spleen sections from WT, $p27^{Kip1-/-}$, $p130^{-/-}$, and $p27^{Kip1-/-}$; $p130^{-/-}$ DKO mice were stained with specific antibodies against B220 (B cells), CD3 (T cells), Ter-119 (erythroid progenitors), and Gr1 (monocytes plus macrophages). Representative sections (magnification, ×250) are shown ($n = 6$ for each genotypes stained). Mice genotypes and the antibodies used are indicated. The spleens of $p27^{Kip1-/-}$; $p130^{-/-}$ mice showed increased cell densities and numbers in all four cell lineages studied, consistent with earlier H&E staining (Fig. 3). Scale bars, 40 μm.

with our observations with the phosphospecific pRB antibodies.

An increase in CDK2 activity in the splenic B220$^+$, CD3$^+$, Ter-119$^+$, and Gr1$^+$ cells of p27^{Kip1}- and p130-deficient mice. To investigate the hematopoietic cell type(s) that contributed to the increase in CDK2 activity in the spleens of the $p27^{Kip1-/-}$; $p130^{-/-}$ mice, we purified Ter-119$^+$, B220$^+$, CD3$^+$, and Gr1$^+$ cells from the four splenic lineages and studied the CDK2 activity by Western blot analysis using anti-phospho-pRB T821 antibodies and by immunoprecipitation kinase assays. Western blot analysis demonstrated that the CDK2 activity was up-regulated in the cells of $p27^{Kip1-/-}$; $p130^{-/-}$ mice of all four hematopoietic lineages (Ter-119$^+$, B220$^+$, CD3$^+$, and Gr1$^+$) compared with that in the cells of $p27^{Kip1-/-}$, $p130^{-/-}$ and wild-type mice (Fig. 7A). The results also showed that, in general, key cell cycle regulators, including p130, pRB, p27^{Kip1}, and CDK2, in these four cell lineages were expressed in a pattern similar to that of the total splenic lysates. Immunoprecipitation kinase experiments performed with the B220$^+$, CD3$^+$, and Tre-119$^+$ cells showed that, in these three cell lineages, the CDK2-associated kinase activity was up-regulated in the cells of $p27^{Kip1-/-}$; $p130^{-/-}$ mice compared with that in their $p27^{Kip1-/-}$, $p130^{-/-}$ and wild-type counterparts (Fig. 7B). However, we failed to perform successful immunoprecipitation kinase studies with Gr1+ cells, and this was most likely due to the limited numbers of cells purified. Nevertheless, together, the Western blotting and immunoprecipitation kinase results clearly indicated that the CDK2 activity is elevated in the cells of $p27^{Kip1-/-}$; $p130^{-/-}$ mice in all four hematopoietic cell lineages and supported the notion that p27^{Kip1} and p130 cooperate to repress CDK2 activity in these cells.

CDK2 is associated with p130 in the p27^{Kip1}-null cells and vice versa. To investigate the compensatory mechanism that represses the CDK2 activity in the $p27^{Kip1}$- and/or *p130*-deficient cells, we then immunoprecipitated CDK2 from splenocytes and thymocytes and analyzed the associated CKI by Western blotting (Fig. 8). The experiments showed that p27^{Kip1} associated with the CDK2 complexes in both wild-type and $p130^{-/-}$ cells (Fig. 8A). However, in the wild-type cells, a

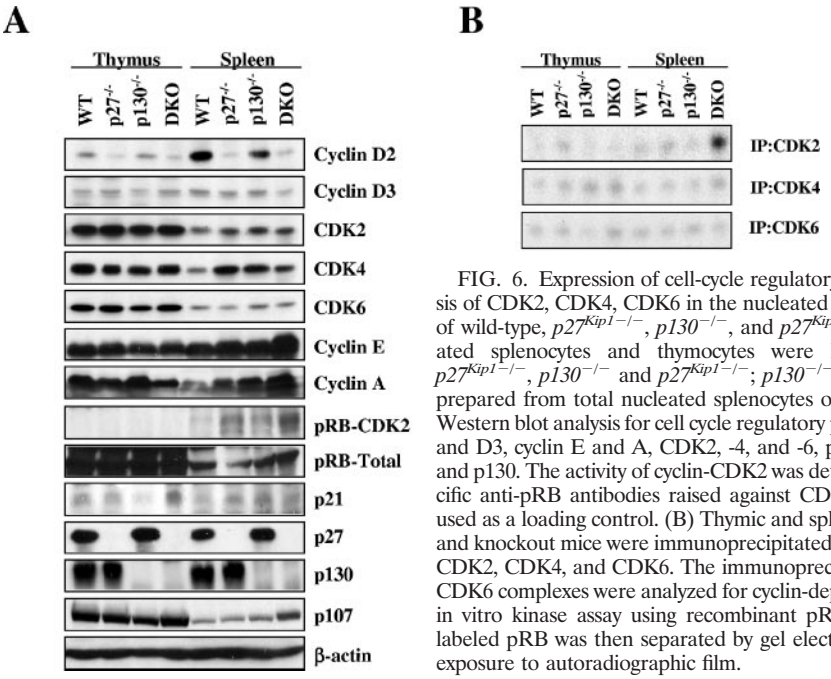

FIG. 6. Expression of cell-cycle regulatory proteins and kinase analysis of CDK2, CDK4, CDK6 in the nucleated splenocytes and thymocytes of wild-type, $p27^{Kip1-/-}$, $p130^{-/-}$, and $p27^{Kip1-/-}$; $p130^{-/-}$ mice. Nucleated splenocytes and thymocytes were harvested from wild-type, $p27^{Kip1-/-}$, $p130^{-/-}$ and $p27^{Kip1-/-}$; $p130^{-/-}$ mice. (A) Lysates (30 μg) prepared from total nucleated splenocytes or thymocytes were used for Western blot analysis for cell cycle regulatory proteins, including cyclin D2 and D3, cyclin E and A, CDK2, -4, and -6, $p27^{Kip1}$, $p21^{Cip1}$, pRB, p107, and p130. The activity of cyclin-CDK2 was determined using phosphospecific anti-pRB antibodies raised against CDK2-specific sites. Actin was used as a loading control. (B) Thymic and splenic cell lysates of wild-type and knockout mice were immunoprecipitated (IP) with antibodies against CDK2, CDK4, and CDK6. The immunoprecipitated CDK2, CDK4, and CDK6 complexes were analyzed for cyclin-dependent kinase activity in an in vitro kinase assay using recombinant pRB as a substrate. The ^{32}P-labeled pRB was then separated by gel electrophoresis and analyzed by exposure to autoradiographic film.

small amount of p130 also bound to CDK2 and the levels of p130 interacting with CDK2 increased when $p27^{Kip1}$ was deleted. We also analyzed whether $p27^{Kip1}$ or p130 was also detected in CDK4 and CDK6 complexes but failed to detect significant levels of $p27^{Kip1}$ or p130 interacting with either CDK4 or CDK6 (Fig. 8B and C). The fact that there was no induction of CDK2 activity in the thymic cell samples prompted us to investigate whether CDK2 also associates with the other pRB-related protein, p107, which has been shown to be able to bind to and inhibit CDK2 kinase complexes (Fig. 8A). The results showed that CDK2 binds to p107 in both the splenic and thymic lysates, suggesting that p107 is also involved in the regulation of CDK2. Notably, there was an increase in p107 interacting with CDK2 in cells with $p27^{Kip1}$ deleted. This indicates that like p130, p107 may also compensate for the absence of $p27^{Kip1}$ to modulate CDK2 activity.

To further confirm these results, we next determined the amount of CDK2 binding to $p27^{Kip1}$ and p130 by Western blotting following immunoprecipitation (Fig. 8D and E). The results showed that, in all wild-type cells, CDK2 binds primarily to $p27^{Kip1}$ and also to a low level of p130, while in all $p27^{Kip1-/-}$ cell types, the majority of CDK2 binds to p130. In the absence of p130, the CDK2 complexes were associated with $p27^{Kip1}$ and, as predicted, no CDK2 was coimmunoprecipitated with antibodies against $p27^{Kip1}$ and p130 in the doubly deficient cells. The differences in the relative signals obtained for $p27^{Kip1}$, p130, or p107 that coprecipitates with CDK2 in spleen relative to thymus in the above-described experiments is explained by the fact that there is less CDK2 in splenocytes. Taken together, these results demonstrate that $p27^{Kip1}$ and p130 each have a role in inhibiting CDK2 activity, and there is an increase in p130 binding to CDK2 in $p27^{Kip1-/-}$ cells compared to that in wild-type cells.

p130 is the CKI binding to CDK2 in splenocytes of $p27^{Kip1-/-}$ mice. While p130 is the major CKI binding to CDK2 in the splenocytes of $p27^{Kip1-/-}$ mice, the experiments described did not address the scenario that another CKI could have a more predominant role in binding to and inhibiting CDK2 in the $p27^{Kip1-/-}$ splenocytes. To investigate this possibility, we performed immunodepletion experiments through serial immunoprecipitation of cell lysates with antibodies against either $p27^{Kip1}$ or p130 (Fig. 9). Three rounds of immunoprecipitation with either the $p27^{Kip1}$ or p130 antibodies completely eliminated CDK2 from the splenocyte lysates. The results also demonstrated that the immunodepletion of $p27^{Kip1}$ from splenocyte lysates of wild-type and $p130^{-/-}$ mice concomitantly removed almost all of the CDK2, whereas the CDK2 complexes in the lysates of $p27^{Kip1-/-}$ and $p27^{Kip1-/-}$; $p130^{-/-}$ mice were unaffected (Fig. 9A). p130 immunodepletion caused a significant reduction of CDK2 protein from the lysates of $p27^{Kip1-/-}$ mice but had little effect on the CDK2 proteins in lysates from wild-type, $p130^{-/-}$, and double-mutant mice (Fig. 9B). Thus, $p27^{Kip1}$ is the major CKI binding to CDK2 in the splenic cells of wild-type and $p130^{-/-}$ mice, whereas p130 is the predominant CKI associated with CDK2 in splenocytes without $p27^{Kip1}$. This result is consistent with the fact that $p27^{Kip1}$ and p130 compensate for each other to regulate CDK2 activity in splenic cells. It was also notable that, after the immunodepletion of $p27^{Kip1}$ and p130, a significant amount of CDK2 was retained in thymus cell lysates, suggesting that only a fraction of the CDK2 complexes was associated with p130 and $p27^{Kip1}$. It is also possible, though unlikely, that most of the CDK2 is not associated with a cyclin; however, without the cyclin regulatory subunit, this pool of CDK2 will be in an inactive form and will not be a target of CDK inhibitors.

***$p27^{Kip1-/-}$; $p130^{-/-}$* splenic B lymphocytes have increased proliferative rates and abilities to enter the cell cycle ex vivo.** It is possible that the increase in cellularity was due to indirect effects from their p130- and p27-null microenvironments in the spleen rather than the deletion of p130 and p27 in these he-

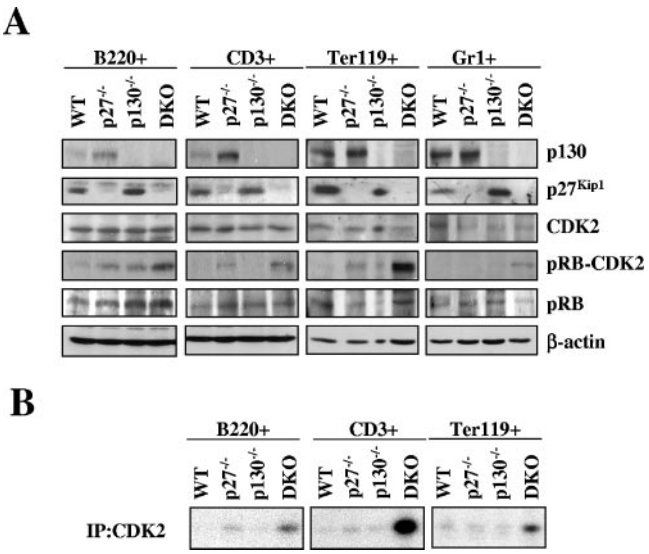

FIG. 7. Expression of cell-cycle regulatory proteins and CDK2 kinase analysis in purified B220$^+$, CD3$^+$, Ter-119$^+$, and Gr1$^+$ splenocytes. Nucleated splenocytes were harvested from wild-type, *p27$^{Kip1-/-}$*, *p130$^{-/-}$*, and *p27$^{Kip1-/-}$*; *p130$^{-/-}$* mice and sorted according to cell surface markers using immunomagnetic microbeads against B220 (B cells), CD3 (T cells), Gr1 (monocytes plus macrophages), and Ter-119 (erythroid progenitors). (A) Lysates (30 μg) prepared from purified B220+, CD3$^+$, Ter-119$^+$, and Gr1$^+$ splenocytes were used for Western blot analysis for cell cycle regulatory proteins, including CDK2, p27^{Kip1}, pRB, and p130. The activity of CDK2 was determined using phosphospecific anti-pRB antibodies raised against CDK2-specific sites. Actin was used as a loading control. (B) Splenic cell lysates of wild-type and knockout mice immunoprecipitated (IP) with antibodies against CDK2 were analyzed for cyclin-dependent kinase activity in an in vitro kinase assay using recombinant pRB as a substrate. The ^{32}P-labeled pRB was then separated by gel electrophoresis, transferred onto a nitrocellulose membrane, and analyzed by exposure to autoradiographic film.

mopoietic cells. To investigate this possibility, we isolated small, dense (resting) B cells from the double- and single-knockout mice and monitored their proliferative rates ex vivo by [^{3}H]thymidine incorporation in response to mitogenic stimulations (Fig. 10). The B cells from wild-type, *p27$^{Kip1-/-}$*, *p130$^{-/-}$*, and *p27$^{Kip1-/-}$*; *p130$^{-/-}$* mice were incubated with optimal concentrations of anti-IgM, anti-CD40, IL-4, anti-IgM and anti-CD40, anti-IgM and IL-4, IL-4 and anti-CD40, or LPS. The results showed that, in most conditions, [^{3}H]thymidine incorporation in the B cells of *p130$^{-/-}$* mice is comparable with that in wild-type cells. Higher levels of [^{3}H]thymidine incorporation occurred in the B cells of *p27$^{Kip1-/-}$* mice, which was increased further in the doubly deficient B cells. The majority of the cells entered S phase between 44 and 72 h. It is notable that there was a reduction in [^{3}H]thymidine uptake at 72 h compared with that at 48 h by some of the B cells, especially under strong mitogenic stimulatory conditions (e.g., LPS). This probably reflects the fact that the majority of the cycling cells had already exited/traversed S phase at 72 h under these conditions. The [^{3}H]thymidine incorporation experiments suggested that the B cells of *p27$^{Kip1-/-}$*; *p130$^{-/-}$* doubly deficient mice enter S phase more rapidly (measured ex vivo) than the B cells of *p27$^{Kip1-/-}$* mice, which in turn are more rapid than the B cells of wild-type and *p130$^{-/-}$* mice. It is also notable that there was a small but significant number of B cells of *p27$^{Kip1-/-}$*; *p130$^{-/-}$* mice entering the cell cycle in the absence of mitogenic stimulation, suggesting that normal $G_0 \rightarrow G_1 \rightarrow$S-phase controls are abrogated.

DISCUSSION

It is believed that the CKI p27^{Kip1} sets stoichiometric inhibitory thresholds for proliferation and thereby prevents premature or inappropriate cell cycle entry. Mice deficient for p27^{Kip1} are recognized to develop hyperplasia in multiple cell types and lineages (15, 23, 32). In particular, the increase in the cellularity and weight of hematopoietic organs, such as the thymus and spleen, far exceeds the general increase in body weight, suggesting that p27^{Kip1} is a hematopoietic tissue-specific regulator of hematopoietic cell cycle entry and proliferation. Indeed, p27^{Kip1} provides the major inhibitory control on CDK2 activity in the majority of hematopoietic cells (14, 16, 40).

The lack of overt proliferative phenotypes in the major hematopoietic organs of the *p27$^{Kip1-/-}$* mice also indicates functional redundancy, and compensation exists to prevent excess uncontrolled proliferation (15, 23, 32). Previous studies have shown that the deletion of *p27^{Kip1}* selectively induced the proliferation of hematopoietic progenitor cells in the spleen (15). Our study demonstrated that the knockout of *p27^{Kip1}* also enhanced the cell cycle entry and proliferation of more mature B cells in response to mitogenic stimulations. Previous data demonstrated that *p27^{Kip1}* deletion leads to enhanced mitogen responsiveness in T cells in vitro (20, 30). We showed that this is also true for B cells. In this report, we provided both molecular and genetic evidence for the concept that p130 functions to compensate for the absence of p27^{Kip1} in binding to and inhibiting CDK2 and that p130 is a bona fide CKI in vivo. Our immunoprecipitation and immunodepletion results indicate that the pRB-related protein p130 can compensate for the absence of p27^{Kip1} in binding to and repressing CDK2 in spleen and thymus. This is further supported by the hyperproliferative effects observed in the splenocytes of *p27^{Kip1}* and *p130* double-mutant mice compared with those seen in their *p27$^{Kip1-/-}$* single-mutant counterparts. Our results also indicate that the compensatory mechanism does not involve the classical CKIs p21^{Cip1} and p57^{Kip2} because there was no detectable amount of p21^{Cip1} or p57^{Kip2} binding to the inactive CDK2 in the hematopoietic cells of either quiescent wild-type or *p27$^{Kip1-/-}$* mice (data not shown). Moreover, while p21^{Cip1} expression levels were not elevated in the cells of *p27$^{Kip1-/-}$* mice, p57^{Kip2} is not expressed at significant levels. Indeed, p21^{Cip1} has also been reported to have a positive rather than negative role on hematopoietic cell proliferation. The enhanced cell proliferation status and hyperphosphorylation of pRB in hematopoietic cells have been shown to be associated with an increase in p21^{Cip1} expression level (41). Active CDK complexes containing p21^{Cip1} have been detected, and it has been suggested that p21^{Cip1} may stabilize such complexes. Therefore, p21^{Cip1} may have a role independent of growth arrest in hematopoietic cells (18). Both p27^{Kip1} and p130 have broad antiproliferative effects on a variety of cell types and tissues outside the hematopoietic system. To eliminate the possibility of the p27^{Kip1}- and p130-dependent environment

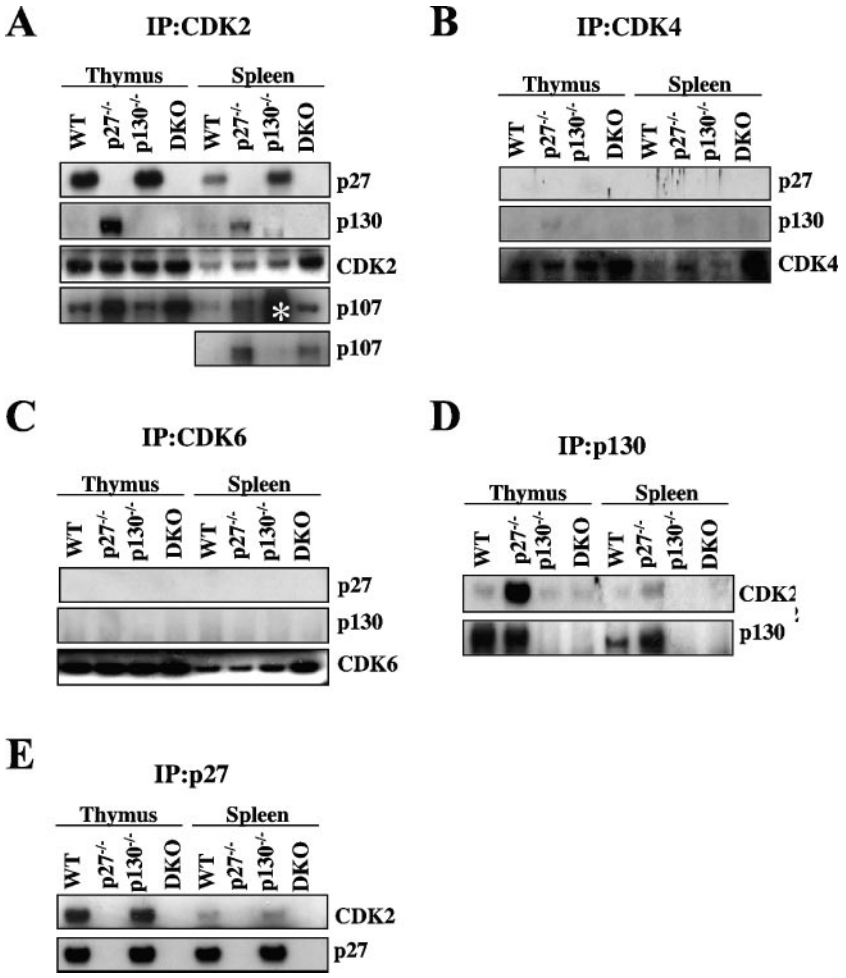

FIG. 8. Immunoprecipitation analysis of CDK2, CDK4, CDK6, p27Kip1, and p130 complexes in wild-type, *p27Kip1−/−*, *p130−/−*, and *p27Kip1−/−*; *p130−/−* mice. Thymic and splenic cell lysates of wild-type and knockout mice were immunoprecipitated (IP) with antibodies against (A) CDK2, (B) CDK4, (C) CDK6, (D) p130, or (E) p27Kip1. The immunoprecipitated CDK2 complexes were analyzed by Western blotting for p27Kip1, p130, and p107. The immunoprecipitated CDK4 and CDK6 complexes were analyzed by Western blotting for p27Kip1 and p130 and the p27Kip1 and p130 complexes for CDK2. The asterisk denotes a spoilt lane, and the immunoprecipitation analysis of CDK2 was repeated (shown underneath).

having an influence on hematopoietic development in these mice, we used B cells as a model system to test their proliferative potential in vitro. The finding that the B cells of *p27Kip1−/−*; *p130−/−* doubly deficient mice are hypersensitive to mitogenic stimulations in vitro supports the idea that the hyperproliferation of splenocytes is not solely a result of the influence of their environment in vivo.

Previous studies have shown that a unique domain within the spacer region of p130 is essential for binding to and inhibiting CDK2 (12, 44). Although the amino acid sequence of this

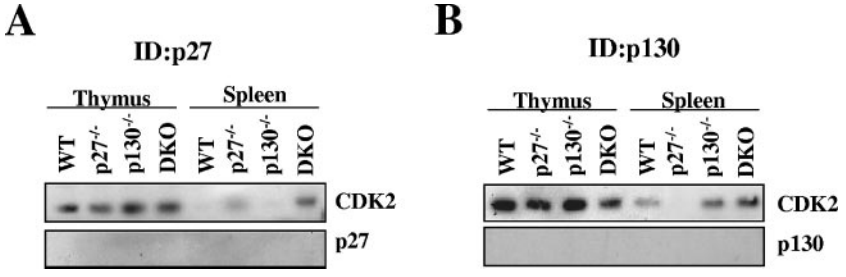

FIG. 9. Immunodepletion analysis of p27Kip1 and p130 complexes in thymi and spleens of wild-type, *p27Kip1−/−*, *p130−/−*, and *p27Kip1−/−*; *p130−/−* mice. Whole-cell extracts were immunodepleted (ID) with three rounds of immunoprecipitation using specific antibodies against (A) p27Kip1 or (B) p130. The resultant supernatants were immunoblotted for CDK2 and p27Kip1 or p130.

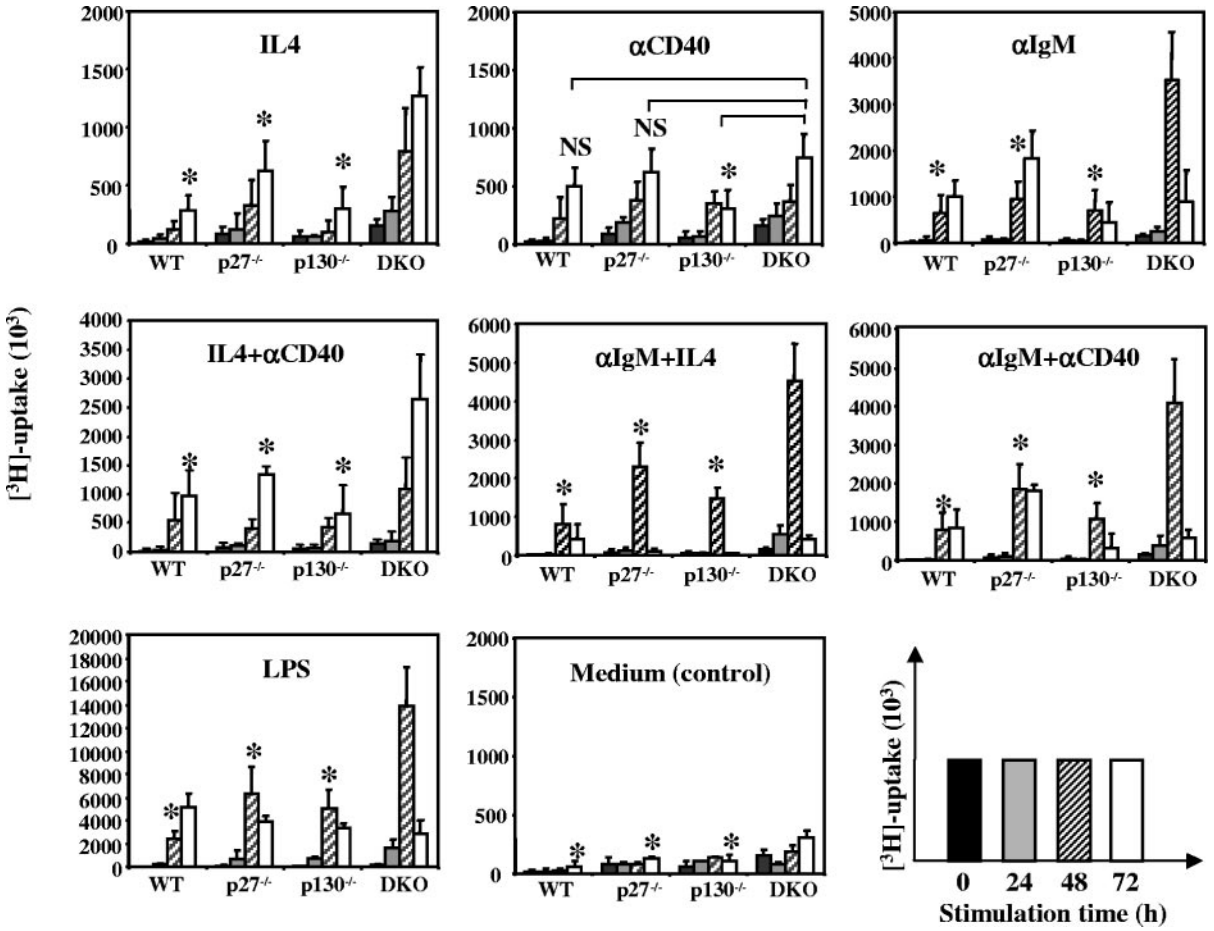

FIG. 10. [^{3}H]thymidine incorporation assay. Small, dense B cells were harvested from the spleens of either wild-type, $p27^{Kip1-/-}$, $p130^{-/-}$, or $p27^{Kip1-/-}$; $p130^{-/-}$ mice and incubated with IL-4, anti (α)-CD40, anti-IgM, IL-4+anti-CD40, IL-4+anti-IgM, anti-IgM+anti-CD40, LPS, or medium only for 0 (black bars), 24 (gray bars), 48 (hatched bars), and 72 (white bars) h. The cells were pulsed with [^{3}H]thymidine for 4 h and harvested, and radioactivity was quantified. The [^{3}H]thymidine uptake was plotted against time, and the result is representative of three individual sets of experiments. Each time point is derived from a triplicate set of results (mean ± SD [error bars]; $n = 3$). Due to the differences in kinetics of cell cycle entry between different treatments, Student t tests were performed on the maximum [^{3}H]thymidine uptake points between the DKO samples and the WT, $p27^{Kip1-/-}$, or $p130^{-/-}$ samples. There is a statistically significant difference in [^{3}H]thymidine uptake between the DKO group and the other genotypes ($P < 0.01$ in response to IL-4, anti-IgM, IL-4+anti-CD40, IL-4+anti-IgM, anti-IgM+anti-CD40, LPS, and medium only but not to anti-CD40). NS, not significant. *, statistically significant ($P \leq 0.01$).

domain is not shared with the pRB-related p107 pocket protein, p107 has also been shown to be able to associate with and repress CDK2 through another p21^{Cip1}-like motif located at the spacer region (2, 44, 47). Another second cyclin-binding site has also mapped to the N-terminal portions of p107 and p130 (2, 44). This N-terminal domain is capable of inhibiting cyclin-cdk2 complexes. It is therefore plausible that p107 can also functionally substitute for the absence of p27^{Kip1} and p130 in the p27^{Kip1} and p130 doubly deficient cells. In agreement with this idea, our data demonstrate that p107, like p130, can also bind to CDK2 in both spleen and thymus. Interestingly, in particular in the thymus, the amount of p107 binding to CDK2 increases when p27^{Kip1} is absent, indicating that p107 might also functionally compensate for p27^{Kip1} in repressing CDK2. This compensatory mechanism can help to explain for the lack of a significant proliferative phenotype in the *p130* and *p27^{Kip1}* doubly deficient thymocytes and, possibly, for the absence of even more severe disorders in the splenocytes. In the thymocytes, the expression level of p107 is high compared with that in the splenocytes, thus allowing p107 to play a more prominent role than that of p130 in inhibiting CDK2 activity. This may explain the lack of excessive thymocyte proliferation when both p130 and p27^{Kip1} are lost and is supported by the finding that high levels of p107 are associated with CDK2 in the thymus but not the spleen. The high intrinsic levels of CDK2 could also potentially exacerbate the situation in the thymocytes. Indeed, functional compensation between pRB family proteins has previously been documented in vivo, but it has mostly centered on their roles in repressing E2F activity (6, 7, 11, 36). These findings also suggest that the ability of p130 to compensate for the absence of p27^{Kip1} is tissue and cell type specific, depending on the relative intrinsic cellular abundance of p130 and p107.

It is notable that the hyperproliferative phenotype of *p27^{Kip1}* and *p130* double deletion affects only splenic cells and not thymocytes. This can be explained by the fact that the majority

(>95%) of cells in the thymus are of one cell type, $CD4^+$ or $CD8^+$ T cells, and this one cell type contributes significantly to the phenotype of the total thymic cell population. Conversely, the fact that hyperproliferative effects of *p27Kip1* and *p130* deletion affect multiple splenic cell types (i.e., B and T lymphocytes, erythroid cells, monocytes, and macrophages) illustrates that this compensatory mechanism that exists between *p27Kip1* and *p130* is common in many different hematopoietic cells. Our data therefore suggest that cell types, such as splenocytes, that intrinsically express low amounts of p107 are largely dependent on p130 for the regulation of the CDK2 activity in the absence of $p27^{Kip1}$. It is also notable that the deletion of both $p27^{Kip1}$ and p130 has a more significant effect on the proliferation of the myeloid populations (erythroid cells, monocytes, and macrophages) than on the lymphoid cells (B and T cells). This probably reflects that the erythroid cells, monocytes, and macrophages or their progenitors are more dependent on $p27^{Kip1}$ and p130 in their cell cycle entry control compared with the splenic T and B cells, and this can be governed by the relative expression levels of different CKIs in each cell type.

The biological significance of $p27^{Kip1}$ and p130 having overlapping functions is unclear. Our previous data suggested that the repression of CDK2 activity by $p27^{Kip1}$ is required for the G_1 arrest induced by the inhibition of the phosphoinositide 3-kinase (PI3K) pathway (10). We also showed that the reason why $p27^{Kip1-/-}$ MEFs still entered cell cycle arrest after treatment with the PI3K inhibitor LY294002 is due to a compensatory mechanism by which p130 functionally substitutes for $p27^{Kip1}$ deficiency (10). These results indicate that both $p27^{Kip1}$ and p130 are downstream effectors of the PI3K pathway. In support of this indication, we have recently demonstrated that both $p27^{Kip1}$ and p130 are direct gene targets of the FOXO subfamily of transcription factors (13, 24). The inhibition of the PI3K pathway induces a cell cycle arrest mediated by $p27^{Kip1}$ and p130. The fact that both $p27^{Kip1}$ and p130 function downstream of the same regulatory pathway may well be important. One possible explanation is that this compensatory mechanism exists to ensure that the cell cycle regulatory function of the PI3K pathway is intact even if one effector becomes inactivated. This compensatory mechanism may provide an essential proliferation control in settings where $p27^{Kip1}$ is not expressed at normal levels, as is the case in many human tumors and hyperplasia. The cooperation between these two cell cycle inhibitors is further supported by a recent study from another group of researchers who also generated mice lacking *p130* and *p27Kip1* and showed that p130 and $p27^{Kip1}$ cooperate to control the mobilization of angiogenic progenitors from bone marrow (42).

In summary, we show that p130 and $p27^{Kip1}$ cooperate to regulate hematopoietic cell proliferation. Our data also indicate that p130 is a bona fide cyclin-dependent kinase inhibitor in vivo and functions to compensate for the absence of $p27^{Kip1}$ to inhibit CDK activity. Ultimately, the generation of mice deficient for *p27Kip1*, *p130*, and/or *p107* will be required to understand the compensatory mechanisms that exist to control cell cycle entry and progression in hematopoietic cells in different organs in vivo.

ACKNOWLEDGMENTS

We thank Nicola Hardwick for her help on [^{3}H]thymidine and cell cycle analyses.

Inês Soeiro is a recipient of a fellowship from Fundação para a Ciência e a Tecnologia, Portugal. Azim Mohamedali, Nicholas Lea, and Stephen Orr were supported by the Charles Wolfson Charitable Trust. Shaun Thomas's work is supported by the Leukemia Research Fund and the Charles Wolfson Charitable Trust. David Mann and Emma Child were funded by the BBSRC. Eric Lam's work is supported by Leukemia Research Fund and Cancer Research UK.

REFERENCES

1. **Bankfalvi, A., H. Navabi, B. Bier, W. Bocker, B. Jasani, and K. W. Schmid.** 1994. Wet autoclave pretreatment for antigen retrieval in diagnostic immunohistochemistry. J. Pathol. **174:**223–228.
2. **Castano, E., Y. Kleyner, and B. D. Dynlacht.** 1998. Dual cyclin-binding domains are required for p107 to function as a kinase inhibitor. Mol. Cell. Biol. **18:**5380–5391.
3. **Cheng, M., P. Olivier, J. A. Diehl, M. Fero, M. F. Roussel, J. M. Roberts, and C. J. Sherr.** 1999. The p21(Cip1) and p27(Kip1) CDK 'inhibitors' are essential activators of cyclin D-dependent kinases in murine fibroblasts. EMBO J. **18:**1571–1583.
4. **Cheng, T., N. Rodrigues, D. Dombkowski, S. Stier, and D. T. Scadden.** 2000. Stem cell repopulation efficiency but not pool size is governed by p27(kip1). Nat. Med. **6:**1235–1240.
5. **Cheng, T., N. Rodrigues, H. Shen, Y. Yang, D. Dombkowski, M. Sykes, and D. T. Scadden.** 2000. Hematopoietic stem cell quiescence maintained by p21cip1/waf1. Science **287:**1804–1808.
6. **Classon, M., B. K. Kennedy, R. Mulloy, and E. Harlow.** 2000. Opposing roles of pRB and p107 in adipocyte differentiation. Proc. Natl. Acad. Sci. USA **97:**10826–10831.
7. **Classon, M., S. Salama, C. Gorka, R. Mulloy, P. Braun, and E. Harlow.** 2000. Combinatorial roles for pRB, p107, and p130 in E2F-mediated cell cycle control. Proc. Natl. Acad. Sci. USA **97:**10820–10825.
8. **Coats, S., P. Whyte, M. L. Fero, S. Lacy, G. Chung, E. Randel, E. Firpo, and J. M. Roberts.** 1999. A new pathway for mitogen-dependent cdk2 regulation uncovered in p27(Kip1)-deficient cells. Curr. Biol. **9:**163–173.
9. **Cobrinik, D., M. H. Lee, G. Hannon, G. Mulligan, R. T. Bronson, N. Dyson, E. Harlow, D. Beach, R. A. Weinberg, and T. Jacks.** 1996. Shared role of the pRB-related p130 and p107 proteins in limb development. Genes Dev. **10:**1633–1644.
10. **Collado, M., R. H. Medema, I. Garcia-Cao, M. L. Dubuisson, M. Barradas, J. Glassford, C. Rivas, B. M. Burgering, M. Serrano, and E. W.-F. Lam.** 2000. Inhibition of the phosphoinositide 3-kinase pathway induces a senescence-like arrest mediated by p27Kip1. J. Biol. Chem. **275:**21960–21968.
11. **Dannenberg, J. H., L. Schuijff, M. Dekker, M. van der Valk, and H. te Riele.** 2004. Tissue-specific tumor suppressor activity of retinoblastoma gene homologs p107 and p130. Genes Dev. **18:**2952–2962.
12. **De Luca, A., T. K. MacLachlan, L. Bagella, C. Dean, C. M. Howard, P. P. Claudio, A. Baldi, K. Khalili, and A. Giordano.** 1997. A unique domain of pRb2/p130 acts as an inhibitor of Cdk2 kinase activity. J. Biol. Chem. **272:**20971–20974.
13. **Dijkers, P. F., R. H. Medema, C. Pals, L. Banerji, N. S. Thomas, E. W.-F. Lam, B. M. Burgering, J. A. Raaijmakers, J. W. Lammers, L. Koenderman, and P. J. Coffer.** 2000. Forkhead transcription factor FKHR-L1 modulates cytokine-dependent transcriptional regulation of $p27^{KIP1}$. Mol. Cell. Biol. **20:**9138–9148.
14. **Ezoe, S., I. Matsumura, Y. Satoh, H. Tanaka, and Y. Kanakura.** 2004. Cell cycle regulation in hematopoietic stem/progenitor cells. Cell Cycle **3:**314–318.
15. **Fero, M. L., M. Rivkin, M. Tasch, P. Porter, C. E. Carow, E. Firpo, K. Polyak, L. H. Tsai, V. Broudy, R. M. Perlmutter, K. Kaushansky, and J. M. Roberts.** 1996. A syndrome of multiorgan hyperplasia with features of gigantism, tumorigenesis, and female sterility in p27(Kip1)-deficient mice. Cell **85:**733–744.
16. **Furukawa, Y.** 2002. Cell cycle control genes and hematopoietic cell differentiation. Leuk. Lymphoma **43:**225–231.
17. **Glassford, J., M. Holman, L. Banerji, E. Clayton, G. G. Klaus, M. Turner, and E. W.-F. Lam.** 2001. Vav is required for cyclin D2 induction and proliferation of mouse B lymphocytes activated via the antigen receptor. J. Biol. Chem. **276:**41040–41048.
18. **Hsieh, F. F., L. A. Barnett, W. F. Green, K. Freedman, I. Matushansky, A. I. Skoultchi, and L. L. Kelley.** 2000. Cell cycle exit during terminal erythroid differentiation is associated with accumulation of p27(Kip1) and inactivation of cdk2 kinase. Blood **96:**2746–2754.
19. **Hsu, S. M., L. Raine, and H. Fanger.** 1981. Use of avidin-biotin-peroxidase complex (ABC) in immunoperoxidase techniques: a comparison between ABC and unlabeled antibody (PAP) procedures. J. Histochem. Cytochem. **29:**577–580.
20. **Huleatt, J. W., J. Cresswell, K. Bottomly, and I. N. Crispe.** 2003. P27kip1

regulates the cell cycle arrest and survival of activated T lymphocytes in response to interleukin-2 withdrawal. Immunology **108:**493–501.
21. **Jarviluoma, A., E. S. Child, G. Sarek, P. Sirimongkolkasem, G. Peters, P. M. Ojala, and D. J. Mann.** 2006. Phosphorylation of the cyclin-dependent kinase inhibitor $p21^{Cip1}$ on serine 130 is essential for viral cyclin-mediated bypass of a $p21^{Cip1}$-imposed G_1 arrest. Mol. Cell. Biol. **26:**2430–2440.
22. **Johnson-Leger, C., J. R. Christenson, M. Holman, and G. G. Klaus.** 1998. Evidence for a critical role for IL-2 in CD40-mediated activation of naive B cells by primary CD4 T cells. J. Immunol. **161:**4618–4626.
23. **Kiyokawa, H., R. D. Kineman, K. O. Manova-Todorova, V. C. Soares, E. S. Hoffman, M. Ono, D. Khanam, A. C. Hayday, L. A. Frohman, and A. Koff.** 1996. Enhanced growth of mice lacking the cyclin-dependent kinase inhibitor function of p27(Kip1). Cell **85:**721–732.
24. **Kops, G. J., R. H. Medema, J. Glassford, M. A. Essers, P. F. Dijkers, P. J. Coffer, E. W.-F. Lam, and B. M. Burgering.** 2002. Control of cell cycle exit and entry by protein kinase B-regulated forkhead transcription factors. Mol. Cell. Biol. **22:**2025–2036.
25. **Lam, E. W.-F., J. Glassford, L. Banerji, N. S. Thomas, P. Sicinski, and G. G. Klaus.** 2000. Cyclin D3 compensates for loss of cyclin D2 in mouse B lymphocytes activated via the antigen receptor and CD40. J. Biol. Chem. **275:**3479–3484.
26. **Lam, E. W.-F., and N. B. La Thangue.** 1994. DP and E2F proteins: coordinating transcription with cell cycle progression. Curr. Opin. Cell Biol. **6:**859–866.
27. **Lea, N. C., S. J. Orr, K. Stoeber, G. H. Williams, E. W.-F. Lam, M. A. Ibrahim, G. J. Mufti, and N. S. Thomas.** 2003. Commitment point during $G_0 \rightarrow G_1$ that controls entry into the cell cycle. Mol. Cell. Biol. **23:**2351–2361.
28. **LeCouter, J. E., B. Kablar, P. F. Whyte, C. Ying, and M. A. Rudnicki.** 1998. Strain-dependent embryonic lethality in mice lacking the retinoblastoma-related p130 gene. Development **125:**4669–4679.
29. **Matsuoka, S., M. C. Edwards, C. Bai, S. Parker, P. Zhang, A. Baldini, J. W. Harper, and S. J. Elledge.** 1995. p57KIP2, a structurally distinct member of the p21CIP1 Cdk inhibitor family, is a candidate tumor suppressor gene. Genes Dev. **9:**650–662.
30. **Mohapatra, S., D. Agrawal, and W. J. Pledger.** 2001. p27Kip1 regulates T cell proliferation. J. Biol. Chem. **276:**21976–21983.
31. **Morel, F., S. Salimi, J. Markovits, T. W. Austin, and I. Plavec.** 1999. Hematologic recovery in mice transplanted with bone marrow stem cells expressing anti-human immunodeficiency virus genes. Hum. Gene Ther. **10:** 2779–2787.
32. **Nakayama, K., N. Ishida, M. Shirane, A. Inomata, T. Inoue, N. Shishido, I. Horii, and D. Y. Loh.** 1996. Mice lacking p27(Kip1) display increased body size, multiple organ hyperplasia, retinal dysplasia, and pituitary tumors. Cell **85:**707–720.
33. **Okada, S., H. Nakauchi, K. Nagayoshi, S. Nishikawa, S. Nishikawa, Y. Miura, and T. Suda.** 1991. Enrichment and characterization of murine hematopoietic stem cells that express c-*kit* molecule. Blood **78:**1706–1712.
34. **Pardee, A. B.** 1989. G_1 events and regulation of cell proliferation. Science **246:**603–608.
35. **Rane, S. G., and E. P. Reddy.** 2002. JAKs, STATs and Src kinases in hematopoiesis. Oncogene **21:**3334–3358.
36. **Ruiz, S., M. Santos, C. Segrelles, H. Leis, J. L. Jorcano, A. Berns, J. M. Paramio, and M. Vooijs.** 2004. Unique and overlapping functions of pRb and p107 in the control of proliferation and differentiation in epidermis. Development **131:**2737–2748.
37. **Sherr, C. J., and J. M. Roberts.** 1999. CDK inhibitors: positive and negative regulators of G_1-phase progression. Genes Dev. **13:**1501–1512.
38. **Sherr, C. J., and J. M. Roberts.** 1995. Inhibitors of mammalian G_1 cyclin-dependent kinases. Genes Dev. **9:**1149–1163.
39. **Steinman, R. A.** 2002. Cell cycle regulators and hematopoiesis. Oncogene **21:**3403–3413.
40. **Steinman, R. A., B. Hoffman, A. Iro, C. Guillouf, D. A. Liebermann, and M. E. el-Houseini.** 1994. Induction of p21 (WAF-1/CIP1) during differentiation. Oncogene **9:**3389–3396.
41. **Taniguchi, T., H. Endo, N. Chikatsu, K. Uchimaru, S. Asano, T. Fujita, T. Nakahata, and T. Motokura.** 1999. Expression of p21(Cip1/Waf1/Sdi1) and p27(Kip1) cyclin-dependent kinase inhibitors during human hematopoiesis. Blood **93:**4167–4178.
42. **Vidal, A., S. Zacharoulis, W. Guo, D. Shaffer, F. Giancotti, A. H. Bramley, C. de la Hoz, K. K. Jensen, D. Kato, D. D. MacDonald, J. Knowles, N. Yeh, L. A. Frohman, S. Rafii, D. Lyden, and A. Koff.** 2005. p130Rb2 and p27kip1 cooperate to control mobilization of angiogenic progenitors from the bone marrow. Proc. Natl. Acad. Sci. USA **102:**6890–6895.
43. **Williams, C. D., D. C. Linch, M. J. Watts, and N. S. Thomas.** 1997. Characterization of cell cycle status and E2F complexes in mobilized CD34+ cells before and after cytokine stimulation. Blood **90:**194–203.
44. **Woo, M. S., I. Sanchez, and B. D. Dynlacht.** 1997. p130 and p107 use a conserved domain to inhibit cellular cyclin-dependent kinase activity. Mol. Cell. Biol. **17:**3566–3579.
45. **Zarkowska, T., and S. Mittnacht.** 1997. Differential phosphorylation of the retinoblastoma protein by G_1/S cyclin-dependent kinases. J. Biol. Chem. **272:**12738–12746.
46. **Zhan, Y., S. Basu, G. J. Lieschke, D. Grail, A. R. Dunn, and C. Cheers.** 1999. Functional deficiencies of peritoneal cells from gene-targeted mice lacking G-CSF or GM-CSF. J. Leukoc. Biol. **65:**256–264.
47. **Zhu, L., E. Harlow, and B. D. Dynlacht.** 1995. p107 uses a p21CIP1-related domain to bind cyclin/cdk2 and regulate interactions with E2F. Genes Dev. **9:**1740–1752.